UNIVERSITY OF CENTRAL OKLAHOMA
Edmond, Oklahoma
Jackson College of Graduate Studies & Research

The Effects of Replicative Senescence and Telomerase on Contraction and Motility of Fibroblasts

A THESIS

SUBMITTED TO THE GRADUATE FACULTY

In partial fulfillment of the requirements

For the degree of

MASTER OF SCIENCE IN BIOLOGY.

By

Joanne Lykins Peterson

Edmond, Oklahoma

2009

The Effects of Replicative Senescence and Telomerase on Contraction and Motility of Fibroblasts

A THESIS
APPROVED FOR THE DEPARTMENT OF BIOLOGY

December 2009

By

Dr. Melville Vaughan, Committee Chairperson

Dr. James Bidlack, Committee Member

Dr. Gloria Caddell, Committee Member

ACKNOWLEDGEMENTS

I would like to express my deepest gratitude to my advisor Dr. Melville Vaughan as he has given me much needed guidance, knowledge and support in this pursuit of my Master's degree. And as his first graduate student, together we have learned the ins and outs of the graduate program at UCO. I would like to extend my thanks to Dr. Gloria Caddell for her help with manuscript suggestions and intense editing as she would make sure I dotted all my i's and crossed all my t's. And to Dr. Bidlack for his advice on improving the manuscript and for statistical help.

I would also like to thank Edana Robinson for all of her help teaching me various lab techniques and initial training on how to enter data into SigmaPlot and Tiffany Palmer for help with making various solutions needed for my experiments. My appreciation to "Grandpa" Dr. Tomasek at OUHSC for providing the cell cultures needed for this project. Thanks go out to Dr. Caire and Dr. Butler for their assistance with statistics and suggesting analyses for these experiments. And thank you to Toby FitzSimons for moral support, textbook usage and the many in-depth conversations that helped me through some of life's more frustrating times.

And last, but certainly not least, family, friends, co-workers and even my high school students who made sacrifices, put up with my moodiness and endured the stress caused by my incessant procrastination while still finding it in their hearts to provide the words of encouragement I needed to complete this goal. Special thanks go to my mother, Reverend Dr. Sue Lykins, whose help with interpretation of data and suggestions on revisions went well above the duties of a mother. And to my husband, David Peterson, for providing unique forms of encouragement, like writing an intriguing story about how I defended my thesis.

Without everyone's love and support this project would have been much harder to complete. From here I can only hope that I have the same assistance, understanding and love when I pursue my PhD as I have had for my Master's degree.

Funding was provided by the Jackson College of Graduate Studies at the University of Central Oklahoma for materials and supplies needed to perform these experiments.

TABLE OF CONTENTS

LIST OF TABLES

LIST OF FIGURES

ABSTRACT

Fibroblasts are important in wound healing as they can create tension, migrate into a wound, and differentiate into myofibroblasts that produce a contractile force to close the wound. Replicative senescence, or the limit of the number of times a cell divides, may influence the ability of the fibroblast to heal the wound. This study was designed to investigate the formation of myofibroblasts, contraction ability and migration rate of three populations of cells derived from the same cell line: 1) those with early population doublings, 2) those with late population doublings and 3) cells that can divide infinitely due to expression of telomerase (hTERT). A significantly higher percent of myofibroblasts was observed in hTERT cells ($p < 0.001$), and treatment with transforming growth factor-β1 produced significantly more myofibroblasts in all three cell ages ($p<0.001$) when cells were plated on coverslips that provided immediate tension. However, in an environment where tension was not immediate, but developed over time, myofibroblast formation and contraction was limited in all cell ages. Migration of fibroblasts was not significantly affected by cell age or presence of telomerase. The addition of telomerase increased myofibroblast formation, limited their contraction and had no effect on their migration, but may have increased proliferation rates. Overall, the results showed that replicative senescence did not have an effect on myofibroblast formation or migration, but could affect contraction rate.

INTRODUCTION

Background

The skin is the largest organ of the body and it provides protection, temperature regulation, signal reception, and help with excretion and/or absorption of substances (Gartner and Hiatt, 2007). It can be divided into two main layers: the epidermis, composed of stratified squamous keratinized epithelial cells; and the dermis, composed of collagen, elastic fibers and various cells such as fibroblasts, mast cells, lymphocytes, macrophages and fat cells. In the dermal layer, fibroblasts are the most abundant cells. They are responsible for making, organizing, and maintaining many components in the extracellular matrix (ECM), such as collagen fibers that allow cells to anchor themselves for movement (Grinnell, 2003). Organization and maintenance of the ECM help to maintain the shape and elasticity of the skin and contribute to distinguishing features such as fingerprints (Gartner and Hiatt, 2007), while degradation of the ECM can result in wrinkling of the skin (West, 1994). This intricate organization also allows for the dynamic series of events that occurs when the skin's protective ability has been compromised by a wound. When the skin has been wounded, a blood clot creates a temporary seal and provides a provisional ECM upon which cells can move (Singer and Clark, 1999). Fibroblasts are important in the next phase of wound healing as they proliferate and migrate into the wounded area (Clark, 1989; Genever et al., 1993; Singer and Clark, 1999) while synthesizing collagen and fibronectin for the new ECM (Clark, 1989). As migration continues, the fibroblasts reorganize the ECM along lines of stress that provide mechanical tension for the cell (Tomasek et al., 2002). When this tension is present, the fibroblast can differentiate into a proto-myofibroblast, characterized by

cytoplasmic actin fibers and demonstrating limited contractile force. Stimulated by growth factors produced by platelets (Assoian et al., 1983) and cells present in the blood clot, further differentiation creates a myofibroblast that can generate a greater contractile force, thereby allowing the wound to fully close (Tomasek et al., 2002). Myofibroblasts have generally been characterized by the presence of α-smooth muscle actin (α-sma) stress fibers similar to those fibers found in smooth muscle cells (Skalli et al., 1986; Darby et al., 1990). These fibers help increase force and develop tension, allowing enough contraction for a wound to completely close. The presence of the cytokine transforming growth factor –β1 (TGF-β1), naturally produced by platelets, can induce this change by increasing the formation of structural elements such as stress fibers, as well as focal adhesions that contain proteins such as vinculin (Vaughan et al., 2000). Finally, TGF-β1 contributes to the production of α-sma (Desmouliere et al., 1993; Desmouliere, 1995; Vaughan et al., 2000). There is limited *in vivo* data about human wound healing. However, in rats TGF-β levels spike shortly after a wounding event, usually within an hour, and then again five days later, demonstrating its importance to wound healing (Yang et al., 1999). Regulation of TGF-β1 production is done by the molecule itself. While TGF-β1 stimulates several factors that are important for a wound to heal, its deposition of the ECM components at a wound site could also be the cause of scarring and fibrosis (Border and Ruoslahti, 1992; Martin, 1997).

Wound healing is further complicated with age and tends to be decreased in older individuals (Ashcroft et al., 2002); therefore there is great interest in how cellular aging may contribute to this difference. Most cells have a limited lifespan and exhibit reproductive and structural changes as they age. Aging of a cell can result from intrinsic

genetic or biological factors or from extrinsic oxidative stress from environmental factors such as UV radiation (Vaughan et al., 2004). Regardless, as fibroblast cells age, they show an increase in the organization of their cytoskeletal components (Wang and Gundersen, 1984). Microtubule organization centers are amplified in late passage (LP) fibroblasts and 10-nm filaments that encircle the nuclei in early passage (EP) fibroblasts appear to become tightly packed in the perinuclear region of LP cells. Actin fibers that are usually fewer in number and scattered in EP cells become greater in number and heterogeneously distributed in LP cells. Cell proliferation or reproduction in EP cells can be characterized by logarithmic growth that eventually slows and then stops as the cell becomes an LP cell (West, 1994). When a cell reaches a point when it will no longer divide it is termed senescent (Hayflick and Moorhead, 1961). The number of senescent cells in mitotic tissue of primates has been shown to increase with the age of an organism. In younger baboons, 3% of dermal fibroblasts showed signs of senescence whereas 30% of the fibroblasts were senescent in older baboons (Jeyapalan et al., 2007). The number of times a cell can divide before becoming senescent varies depending on species and genetic makeup, and a possible process that limits proliferation based on the number of times a cell divides is termed replicative senescence (Campisi, 1997). There is evidence that replicative senescence plays a role in organismal aging. Cells from older donors do not undergo as much proliferation, and show higher senescence-associated markers and decreased telomere length (Jeyapalan and Sedivy, 2008). The ability to perform wound contraction necessary for healing can also change over the life of a cell. There is conflicting evidence about the effects of age on the cell's ability to contract as demonstrated by studies that have shown that as a cell ages, its contraction ability

increases (Gibson et al., 1989), whereas others have shown that the ability to contract decreases (Bell et al., 1979; Kono et al., 1990; Yamato et al., 1992). The changes in the structure of the ECM as aging occurs can affect the cell's ability to contract as aged fibroblasts do not synthesize as much collagen as younger cells (Varani et al., 2006). In the dermis of aged skin, the collagen matrix upon which fibroblasts attach is fragmented and there is an increase in collagen-degrading matrix metalloproteinases-1 (MMP-1) (Fisher et al., 2008; Fisher et al., 2009). Collagen fragmentation makes it difficult for a fibroblast to anchor itself to create tension and under such conditions the fibroblast collapses. In this collapsed state, the fibroblasts produce lower levels of collagen and higher levels of enzymes, like collagenase, that degrade collagen even further. Similarly, fibroblasts that are triggered to become senescent, possibly due to a decrease in telomere length, lose their ability to initiate proliferation and increase the production of collagenase (West, 1994). The increase in senescent cells in aging skin may play a role in delayed wound healing, especially when the absolute number of cells in aging skin is decreased (Ashcroft et al., 2002).

One of the more prominent views on what controls the process of replicative senescence is the length of telomeres (Wright and Shay, 2002). Telomeres are non-coding sections of repeating TTAGGG nucleotide sequences and specific proteins (Cristofalo et al., 2004; Boukamp, 2005; Shay and Wright, 2007). Each time a cell divides, a small portion of the lagging strand of DNA cannot be replicated, causing the telomere to shorten. Continued replication and telomere shortening will lead to growth arrest or replicative senescence when the telomeres finally become too short. Average telomere lengths have been quantified using PCR techniques (Harley et al., 1990). In neonate

dermal fibroblasts, the average length of telomeres was 10 kbp while only 5 kbp when they became senescent; comparing samples from many ages of donors, an inverse relationship between telomere length and age has been found (Lindsey et al., 1991; Slagboom et al., 1994). Non-human primates, such as spider, squirrel and Rhesus monkeys, along with orangutans and pigmy chimpanzees, also show this inverse relationship between telomere length and age (Steinert et al., 2002). These observations correlate with the demonstrated increase of senescent cells in primate tissues (Jeyapalan, 2007) suggesting that a similar phenomenon would be expected in human tissues as aging occurs. When comparing the initial telomere length in human fibroblasts to the number of times the population can divide, there is a strong correlation of replicative capacity to cell age (Allsopp et al., 1992). The shorter the initial telomere, the fewer times the population could double before becoming senescent. An inverse correlation has also been found between the average telomere length and the age of other cells, such as white blood cells (Cawthon et al., 2003; Kimura et al., 2007). The incidence of certain age-related disorders also has been correlated to the length of telomeres. Shorter telomeres have been found in endothelial cells of patients with coronary artery disease (Ogami et al., 2004) and Alzheimer's patients had short telomeres in their T cells (Panossian et al., 2003). Skin fibroblasts in baboons showed an increase in telomere dysfunction with an increase in age when analyzed for biomarkers of cellular senescence such as telomere dysfunction-induced foci (Herbig et al., 2006).

In cells that proliferate continuously, such as stem cells, germ cells and many tumor cells, telomere shortening can be overcome by the up-regulation of the enzyme telomerase. Telomerase is composed of a telomerase RNA component (TERC) and

telomerase reverse transcriptase (TERT; hTERT when referring to human), together creating a complex that can add replicates of the DNA sequence TTAGGG to the ends of telomeres (Shay and Wright, 2007). Experiments have shown that telomerase can circumvent the effects of replicative senescence (Holt et al., 1996; Funk et al., 2000). Cells transduced with hTERT are termed immortal due to their infinite ability to replicate (Hornsby, 2007). Understanding the mechanisms of replicative senescence and the effects of telomerase could lead to a variety of treatments for aging disorders (Hornsby, 2007) as well as treatments for various cancers (Shay and Wright, 2007).

Objectives

This study was designed to evaluate the consequences of replicative senescence on fibroblasts in terms of myofibroblast formation, contraction and rate of migration, all of which play an important role in wound healing. Previously mentioned studies have shown differences in the behavior of cells as they age (Bell et al., 1979; Wang and Gundersen, 1984; Gibson et al., 1989; Kono et al., 1990; Yamato et al., 1992; West, 1994; Ashcroft et al., 2002; Jeyapalan et al., 2007; Varani et al., 2006), whereas others have studied the events of wound healing and factors that can affect that process (Skalli et al., 1986; Clark, 1989; Darby et al., 1990; Border and Ruoslahti, 1992; Desmouliere et al., 1993; Genever et al., 1993; Desmouliere, 1995; Martin, 1997; Singer and Clark, 1999; Yang et al., 1999; Vaughan et al., 2000; Tomasek et al. 2002). The models used in this study investigated the physiological and morphological changes in aging fibroblasts in vitro, and evaluated how these changes may play a role in the three major functions of fibroblasts in the wound healing process. This study also evaluated the effects of telomerase (referred to as hTERT) to determine if the addition of this enzyme to late

passage cells could immortalize these cells, and then determine whether this can change the replicative senescence phenotype with regard to cellular contraction, migration, and ability to form myofibroblasts. The null hypothesis was that there will be no difference among the three cell ages (early passage, late passage, and hTERT) in the percent of myofibroblasts, the ability to contract or migration time. The alternate hypothesis was that there will be a difference among the cell ages in the percent of myofibroblasts, the ability to contract or migration time.

MATERIALS AND METHODS

Cell cultures

IRB approval was obtained prior to experimental procedures (UCO IRB #09083). Fibroblasts were received from the University of Oklahoma Health Sciences Center (OUHSC) where they were isolated from tissues obtained from patients undergoing Carpal Tunnel release; for these studies cells were obtained from the 4th donor (CT4). When the tissue was placed in a culture dish, fibroblasts migrated out of the tissue and were isolated. The *in vitro* age (described as the average number of replications, or population doublings, per cell population) of the CT4 cells at this point was considered zero. The hTERT cells were transduced at OUHSC by incorporating the hTERT gene into viral particles that incorporated the gene into its hosts' DNA along with an antibiotic resistance vector (pBABE puromyocin). Selection of the transduced hTERT cells was performed by growing them in the presence of puromycin until untransduced cells were killed. When the cells were received from OUHSC, they were cultured in Dulbecco's Modified Eagle's Medium (DMEM, Sigma) + 10% Fetal Bovine Serum (FBS) + penicillin/streptomycin/amphotericin (ABAM, Sigma) and kept incubated in tissue culture dishes (100 x 20 mm, Fisher) at 37^{o}C at 5% CO_2 with high humidity. Cells were subcultured at least once every seven days to keep them from becoming quiescent, a reversible state of nondivision.

To determine cell concentration, cells were counted on a cell counting chamber (hemocytometer) prior to each experiment. Then the appropriate amount of cell solution was added to media to obtain the desired concentration for each test. The age of the cells was determined (each time the cells were subcultured) by calculating how many times the

population had doubled (PD). The total number of cells in the culture dish was determined and then divided by the number of cells originally plated in the dish. The log of this number was divided by 0.3 and the resulting figure was added to the starting PD. CT4 cells usually survive in culture to a PD of ~45 (Vaughan MB, personal communication, June 5, 2009). This study evaluated three ages of cells: early passage cells (EPD) with a PD of less than 20, late passage cells (LPD) with a PD greater than 30 (approaching senescence), and hTERT cells with a PD greater than 30 to ensure that a true comparison could be made between LPD and hTERT in order to assess the ability of telomerase to overcome the effects of aging.

Telomere length was not measured in this study. Because studies have shown that telomeres shorten as a cell ages (for review, Shay and Wright, 2007), it was inferred that the telomeres in the LPD cells were shorter than the EPD cells. Studies have also shown that expression of telomerase can lengthen telomeres (Bodnar et al., 1998) so it was assumed that due to the increased telomerase, the hTERT cells were not subject to telomere shortening.

Coverslips

Glass coverslips (12mm round, Fisher Scientific), 12 for each cell age, were placed into wells in a 24 well spot plate (Falcon Multiwell). A cell concentration of $3.0x10^4$ cells was placed in each well with a coverslip, and 1μL of either TGF-β1 or a vehicle (0.1% bovine serum albumin (BSA) in 1X phosphate buffer solution (PBS)) was added to each of the wells (Figure 1a). Cells were incubated at 37°C for two days. This incubation period allowed time for α-sma to form while limiting the time for cell proliferation. After incubation, coverslips were fixed using methanol at -20°C for five

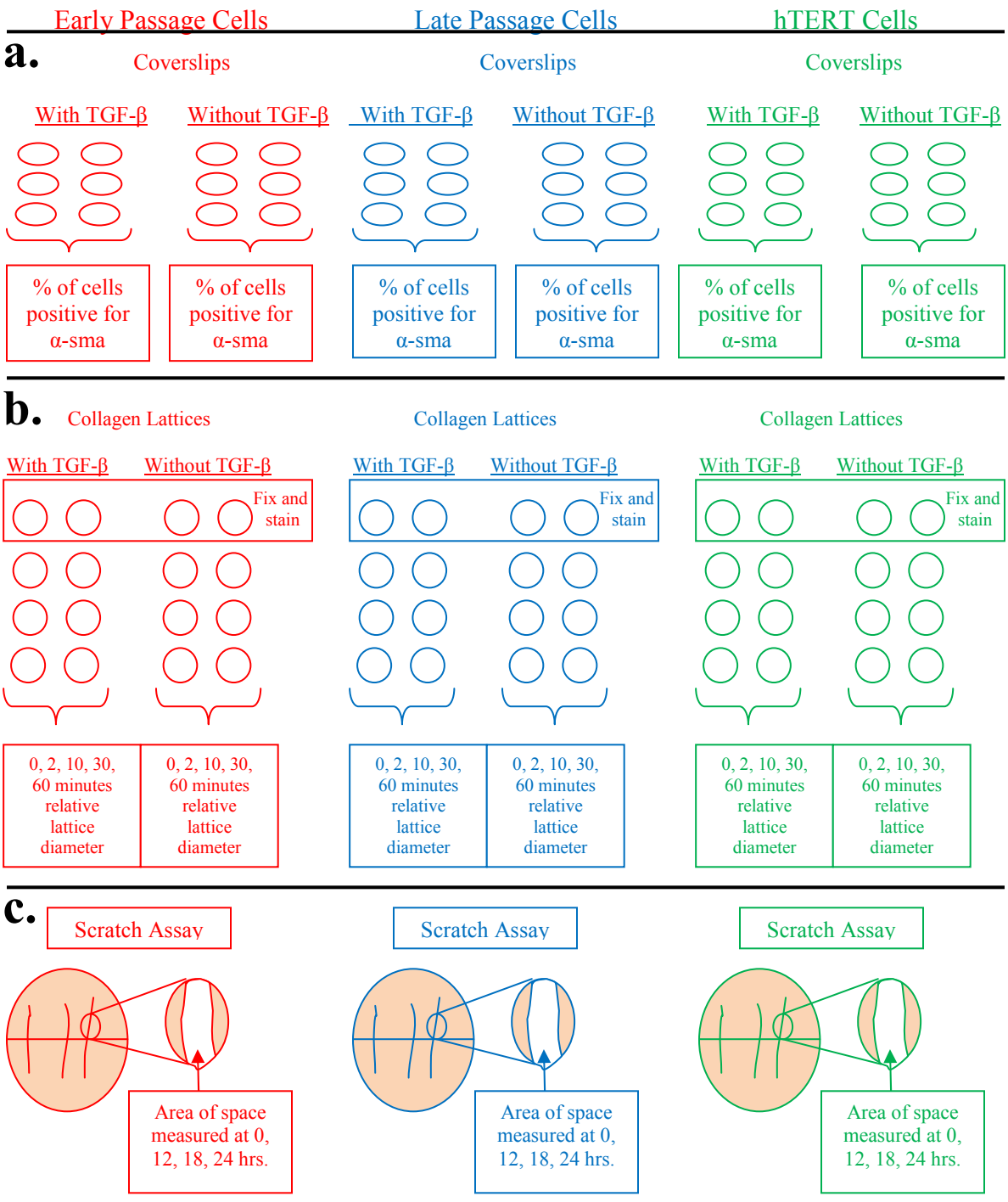

Figure 1. Experimental design.
a. Setup for coverslips provided six replicates in each treatment group for each cell age. **b**. Each collagen lattice design yielded twelve replicates for contraction data (each circle represents two replicates) and two replicates for staining for each cell age. **c**. Each scratch assay yields three replicates, and two assays were done for each cell age.

minutes, rinsed with 1X PBS, and stored in 1X PBS + 0.02% azide until staining.

For each cell age, six coverslips from each treatment group were stained for α-sma using indirect immunofluorescence. The primary antibody used was a mouse anti-α-sma monoclonal antibody (1:500 dilution, clone 1A4, Sigma®). The secondary antibody was goat anti-mouse rhodamine (1:200 dilution, Molecular Probes®). Coverslips were also stained with 4', 6-diamidino-2-phenylindole HCL (DAPI) to visualize the nuclei. Coverslips were then mounted on a microscope slide using 80% glycerol. Each slide was viewed with an Olympus BX-41 microscope equipped with epifluorescence and a digital camera linked to diagnostic software (SPOT Diagnostics™). Using ten to twelve different fields of view on each coverslip, cells were photographed and quantified as α-sma positive or negative (Figure 2). The percentage of myofibroblasts (positive cells) from all fields was determined for each of the six coverslips. The data were then transformed by determining the arcsine of the square root of each percentage. This transformation created more normally distributed data allowing the use of a two-way ANOVA (SigmaPlot 11.0®) to analyze the effects of age and TGF-β1 individually and together. The alpha level was set at 0.05 with degrees of freedom of 35 (n-1, where n = (ages of cells) (groups with or w/o TGF-β1) (replicate means) or (3) (2) (6) =36). Then a Fisher LSD test was used to determine significant pairwise differences among groups.

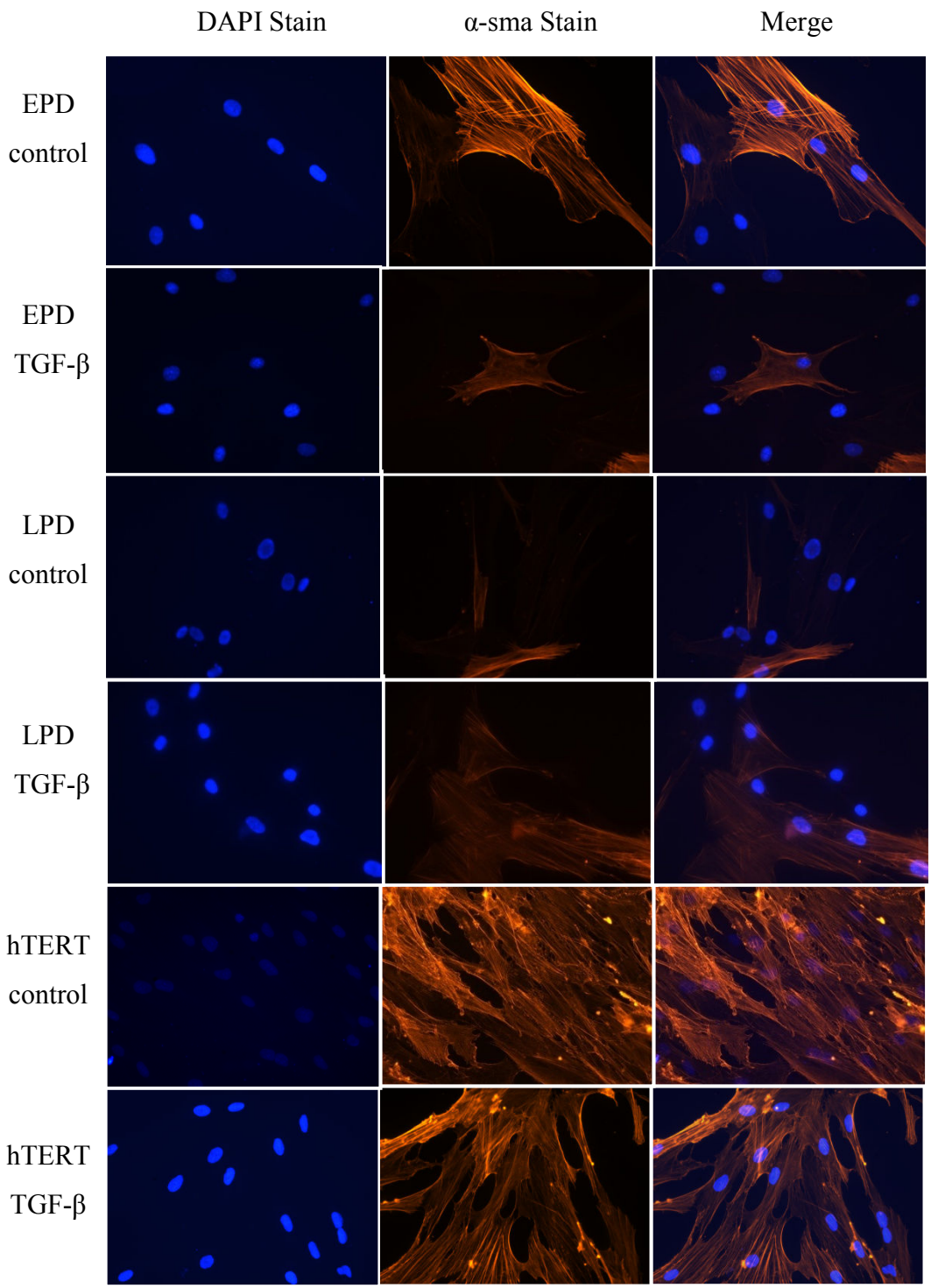

Figure 2. Representative microscopic images to quantify data from stained coverslips. Coverslips were stained with DAPI to visualize and thereby quantify the number of nuclei (cells) in the field of view. α-sma was stained to visualize the stress fibers associated with the myofibroblast phenotype. When the two photos were merged, the number of myofibroblasts was determined by how many nuclei were associated with stress fibers.

Collagen lattices

Cells were mixed into type I collagen (Biocoat; Becton Dickinson) so that the final collagen concentration was 0.69 mg/mL and the final concentration of cells was 1.25×10^5 cells/mL. A 250 µL drop of the collagen/cell mixture was plated onto 40 mm tissue culture dishes (Techno Plastic Products) and incubated at 37°C for one hour to allow the solution to solidify and adhere to the dish. At that time, 2 mL of media (DMEM + 10% FBS + ABAM) with either 1 µL of TGF-β1 or a vehicle (0.1% BSA in 1X PBS) was added to each dish. Dishes were incubated for 2 days to allow α-sma formation with limited proliferation. This incubation time also allowed the fibroblasts to reorganize the lattice and create tension (Tomasek et al., 1992). For each cell age, 28 dishes were prepared (Figure 1b). Fourteen of the 28 dishes were treated with TGF-β1 and 14 with the vehicle (0.1% BSA in 1X PBS). Twelve from each treatment group were released (detached from the dish) and measured. The remaining two lattices from each treatment were preserved in 4% paraformaldehyde (Ultrapure EM Grade, Polysciences®), immersed in 0.25% triton to permeabilize the cell membranes, then stained for α-sma as described with coverslips. Once stained, cells were then identified as α-sma positive or negative and the percentage of myofibroblasts was determined (Figure 3). The data were then transformed by determining the arcsine of the square root of each percentage. This transformation created more normally distributed data allowing the use of a two-way ANOVA (SigmaPlot 11.0®) to analyze the effects of age and TGF-β1 individually and together. The alpha level was set at 0.05 with degrees of freedom of 11 (n-1, where n = (ages of

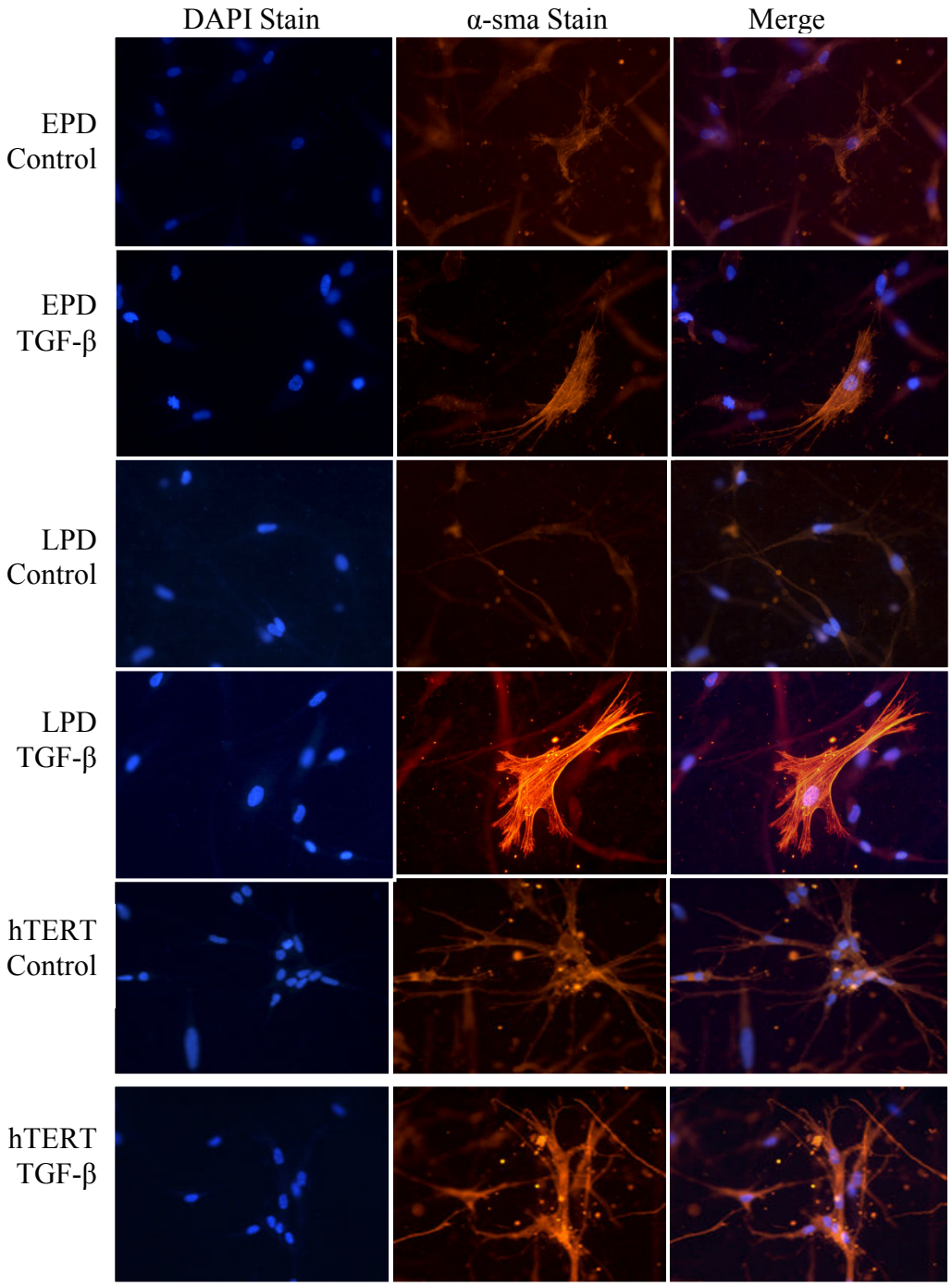

Figure 3. Representative microscopic images to quantify data from stained lattices. Cells were stained with DAPI to visualize and count nuclei (cells). They were also stained for α-sma stress fibers that are characteristic of a myofibroblast phenotype. Nuclei associated with stress fibers were counted as positive and nuclei with no distinct stress fibers were counted as negative.

cells) (groups with or w/o TGF-β1) (replicate means) or (3) (2) (2) = 12). A Fisher LSD test was used to determine significant pairwise differences among groups.

Before releasing a lattice, the initial diameter of the collagen lattice was measured by placing the dish on a ruler and reading it through a Baush & Lomb stereoscope. The lattice was gently lifted at the edge using a probe and then completely released from the dish by pipetting media underneath the loose edge (Tomasek et al., 1992). The diameter of the lattice was recorded at 2, 10, 30 and 60 minutes after release. Due to the variability of the initial lattice diameters, the relative diameter change was used for data comparison and was calculated by dividing the diameter of the lattice at each time point by the initial diameter of the lattice. For each cell age, data were collected from twelve lattices of each treatment group and were analyzed using a two-way ANOVA (SigmaPlot 11.0®) on each of the time points (2, 10, 30, 60 minutes). Alpha level was set at 0.05 and degrees of freedom of 71 (n-1, where n = (ages of cells) (groups with or w/o TGF-β1) (replicates) or (3) (2) (12) = 72). A Fisher LSD test was used to determine significant pairwise differences among groups.

Scratch Assay

Cells were plated in tissue culture dishes (TPP 40 mm) and allowed to become greater than 90% confluent (Denker and Barber, 2002). On the bottom of the plate, a reference line was drawn across the diameter and three scratches were made perpendicular to the line with a 200μL pipet tip (Figure 4). This was done with two dishes to yield six replicates. Photographs of each scratch were taken above or below the reference line at 0, 12, 18 and 24 hours. Each photograph was then used to determine the area of the wound at that time by drawing a line around the perimeter of the open wound

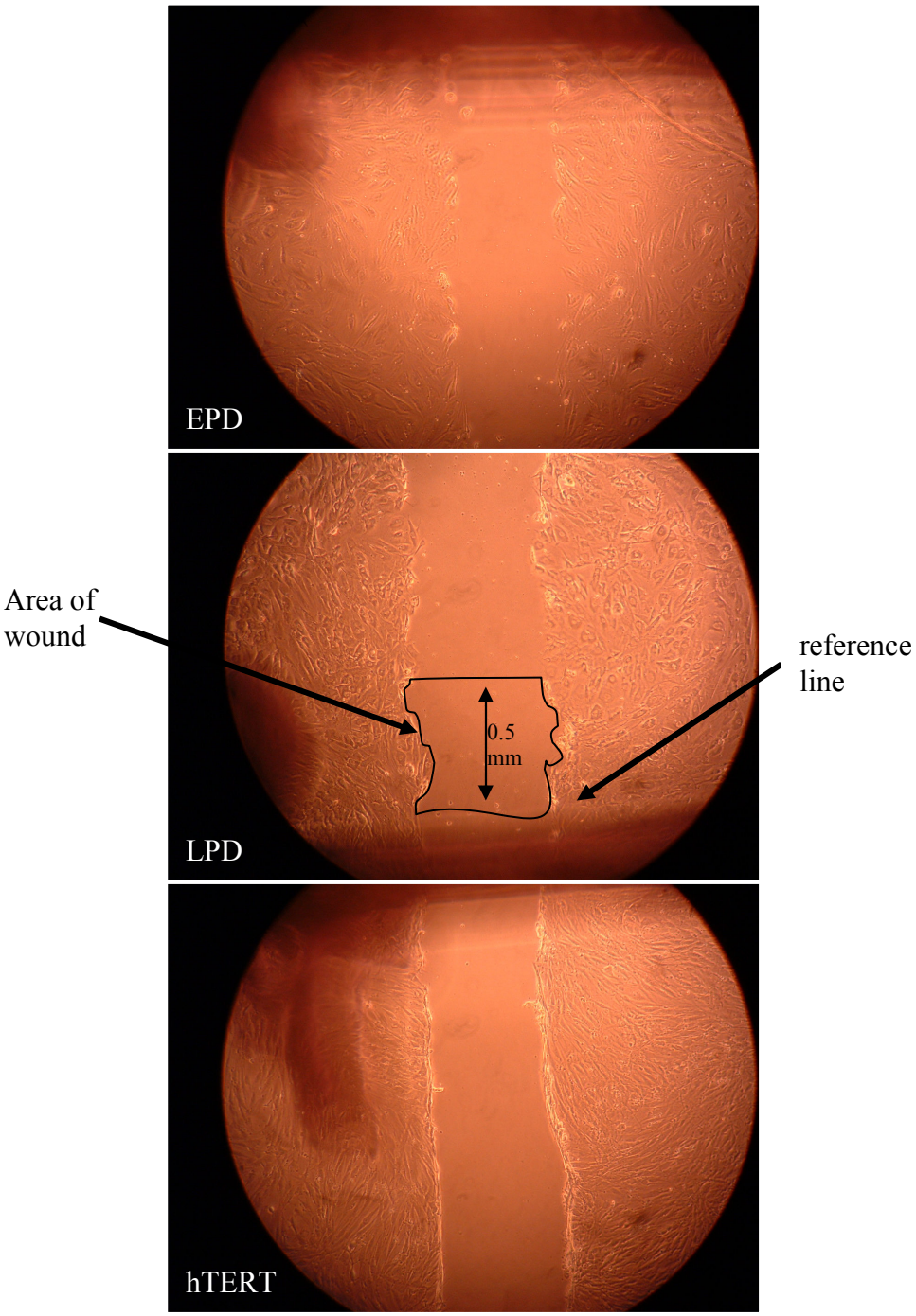

Figure 4. Photographs of the initial wound of scratch assays. Subsequent photos are not displayed since reduction in the size of the image does not provide clarity of the cells or wound edges. Area of the wound was measured as the open wound area that occurs from the reference line out to 0.5 mm.

area and calculating that area (mm^2) using ImageJ software. The wound area was defined starting at the reference line and moving 0.5 mm out from that point to ensure similar areas were being measured (Figure 4). For all three cell ages, the relative decrease in the area at each time marker was analyzed using a two-way ANOVA (SigmaPlot 11.0®). The alpha level was set at 0.05 with degrees of freedom of 53 (n-1, where n = (ages of cells) (time periods) (replicates) or (3) (3) (6) = 54). A Fisher LSD test was used to determine significant pairwise differences among groups.

Cell Count

In the collagen lattice and coverslip tests, proliferation may affect the results (Vaughan et al., 2000; Tomasek et al., 1992). While analyzing the tests, the number of cells counted was recorded, as well as the number of different field of views (fov) analyzed. While this did not give a specific cell concentration, a comparison of the average number of cells per fov was used to determine whether any group had a larger mean number of cells. The mean number of cells per fov was analyzed using a two-way ANOVA (SigmaPlot 11.0®). For coverslips, the alpha level was set at 0.05 with degrees of freedom of 35 (n-1, where n = (ages of cells) (treatment groups) (replicates) or (3) (2) (6) = 36). For collagen lattices, the alpha level was set at 0.05 with degrees of freedom of 11 (n-1, where n = (ages of cells) (treatment groups) (replicates) or (3) (2) (2) = 12). A Fisher LSD test was used to determine significant pairwise differences among groups.

RESULTS

Coverslips

Percentage of Myofibroblasts

Of the early passage cells (EPD) in the control group, 26.2% were myofibroblasts as compared to 71.9% in the TGF-β group (Figure 5). Of the late passage cells (LPD) in the control group, 25.6% were myofibroblasts compared to 63.8% in the TGF- β group. Of the cells transduced with telomerase (hTERT), 80.5% were myofibroblasts in the control group and 93.9% in the TGF-β group. Raw data can be found in the Appendix.

A Shapiro-Wilk test for normality and a test for equality of variances was run. A p value of greater than 0.05 indicates that data are distributed normally and variance in the groups are equal. Both normality ($p = 0.524$) and equality ($p = 0.149$) were found. A two-way analysis of variance (ANOVA) was conducted to evaluate the effects of cell age and TGF-β1 treatment on the development of myofibroblasts. The levels of cell age were early population doubling (EPD), late population doubling (LPD), and the cells transduced with telomerase (hTERT). The levels of treatment were no treatment (control) and TGF-β1 treatment (TGF). Significant differences were found among cell ages $F(2,30) = 41.092$, $p < 0.001$, and drug treatment, $F(1,30) = 59.224$, $p < 0.001$. A significant interaction was found between the cell age and treatment, $F(2,30) = 3.512$, $p = 0.043$ (Table 1).

Fisher LSD across-group tests showed a significant difference between the percent of myofibroblasts present in the control group between hTERT and EPD ($p < 0.001$) and hTERT and LPD ($p < 0.001$). The hTERT cells had significantly higher percentages of myofibroblasts than both EPD and LPD. There was not a significant

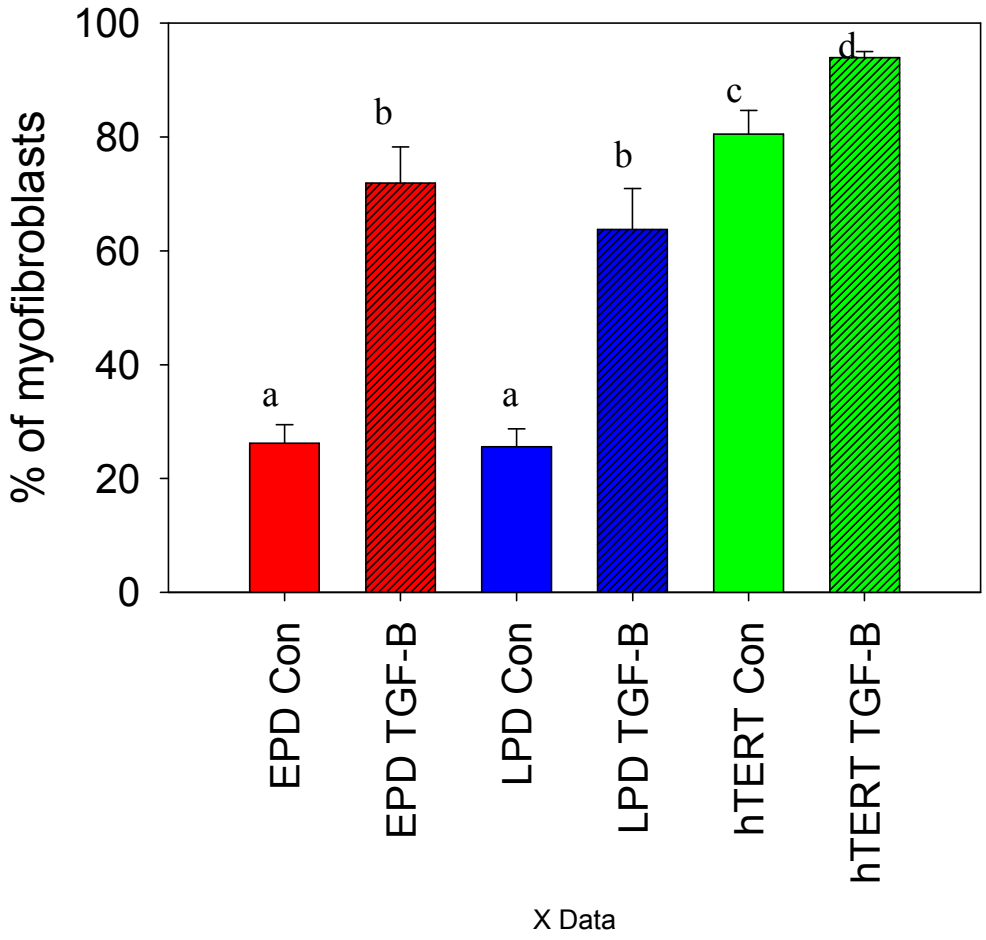

Figure 5. Percentage of myofibroblasts found on coverslips. In all three cell ages, there was a larger percentage of myofibroblasts found in the TGF-β groups. Among the control groups, EPD and LPD cells maintained a similar number of myofibroblasts whereas the hTERT cells were significantly higher. A similar trend appeared in the TGF-β groups, with the hTERT cells having more myofibroblasts than the EPD and LPD cells. Bars with the same letter are not significantly different.

Table 1. Two-way ANOVA results table for myofibroblast formation on coverslips. A P value less than 0.05 shows significance. There was a significant difference in the cell ages, as well as the experimental groups. A Fisher LSD test shows among cell ages, the hTERT cells were different from the EPD and LPD cells, and the TGF-β groups were different from the control groups.

Source of variation	**DF**	**SS**	**MS**	**F**	**P**
Cell Age	2	1.749	0.875	41.092	<0.001
Treatment Group	1	1.261	1.261	59.224	<0.001
Cell Age x Treatment	2	0.150	0.0748	3.512	0.043
Residual	30	0.6.9	0.0213		
Total	35	3.798	0.109		

difference in percentage of myofibroblasts in the control group between EPD and LPD, (p=.928).

These same differences were found in the TGF-β1 groups using Fisher LSD across-group treatment tests. There were significant differences in the percentage of myofibroblasts between the hTERT and EPD ($p < 0.001$) and hTERT and LPD ($p = 0.002$). The hTERT cells again had significantly higher percentages of myofibroblasts then EPD and LPD. There was not a significant difference between EPD and LPD ($p = 0.226$).

Fisher LSD within-group tests showed a significant difference for treatment in all cell ages, EPD ($p < 0.001$) LPD ($p < 0.001$), and hTERT ($p = 0.05$). All three cell ages had a significant increase in number of myofibroblasts when given TGF- β1 (Figure 5).

Cell Count

When quantifying EPD cells within the control group, 712 cells were counted within 72 different fields of view (fov) from 6 coverslips yielding a mean of 9.89 cells/fov (Figure 6). Within the EPD TGF-β group, 713 cells were counted in 72 fov from 6 coverslips yielding a mean of 9.90 cells/fov. When quantifying LPD cells within the control group, 748 cells within 72 different fov from 6 coverslips gave a mean of 10.39 cells/fov. Within the LPD TGF-β group, 687 cells were counted in 72 fov from 6 coverslips giving a mean of 9.54 cells/fov. When quantifying hTERT cells within the control group, 1023 cells within 60 different fov from 6 coverslips gave a mean of 17.05 cells/fov. Within the hTERT TGF-β group, 891 cells were counted in 60 fov from 6 coverslips giving a mean of 14.85 cells/fov. Raw data can be found in the Appendix.

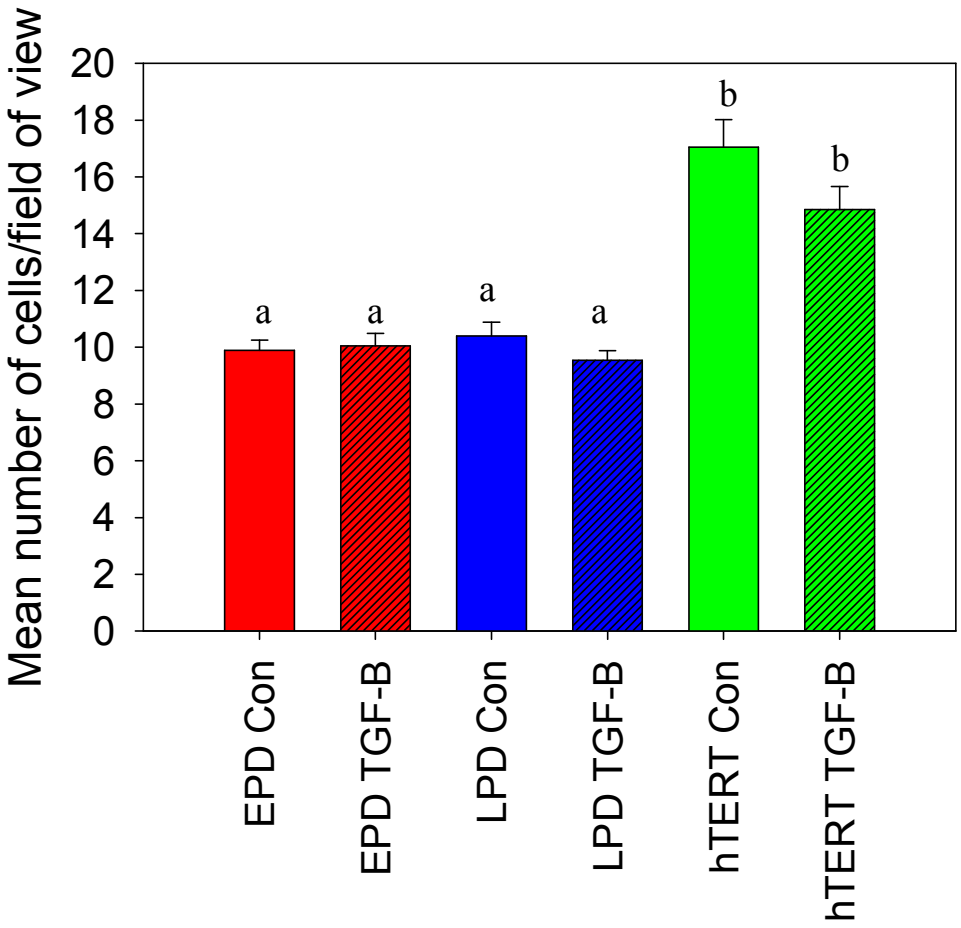

Figure 6. Effect of cell age and treatment on mean number of cells on coverslips. All coverslips were originally plated with the same concentration of cells (0.30×10^5 cells). Proliferation effects were estimated by comparing the mean number of cells per field of view observed. EPD and LPD coverslips maintained similar cell counts whereas hTERT cells had a higher number of cells. Bars with the same letter are not significantly different.

A two-way ANOVA was conducted to evaluate the effects of cell age and TGF-β1 treatment on the total number of cells present. The levels of cell age were early population doubling (EPD), late population doubling (LPD), and the cells transduced with telomerase (hTERT). The levels of treatment were no treatment (control) and TGF-β1 treatment (TGF). A significant difference was found for the main effect of cell age, $F(2,30) = 20.37$, $p < 0.001$. The sub effect of TGF- β1 treatment was not significant, $F(1,30) = 1.293$, $p = 0.0264$. No interaction was found between cell age and TGF- β1 treatment, $F(2,30) = 0.525$, $p = 0.597$ (Table 2).

Fisher LSD across-group tests showed a significant difference in cell number between hTERT and the EPD, ($p < 0.001$) and the hTERT and LPD ($p < 0.001$). There was a significantly greater number of hTERT cells present than EPD and LPD cells. The EPD and LPD were not significantly different ($p = 0.950$) (Figure 6).

Collagen Lattices

Percentage of Myofibroblasts

Non released lattices were stained after two days and then analyzed for myofibroblasts by counting the number of nuclei in a field of view then correlating them to stress fibers. The percentage of cells positive for α-sma in the EPD lattices was 1.2% in the control group and 2.1% in the TGF-β group (Figure 7). In the LPD lattices there were 0.9% in the control group and 1.6% in the TGF-β group. There were 3.1% in the hTERT control group versus 3.2% in the hTERT TGF-β group. Raw data can be found in the Appendix.

Table 2. Two-way ANOVA table for cell number on coverslips. A P value less than 0.05 shows significance. There was a significant difference among cell ages but no significant difference between the treatment groups. No significant interaction occurred. A Fisher LSD test shows that among the cell ages, the number of hTERT cells was significantly higher than the EPD and LPD cells.

Source of variation	**DF**	**SS**	**MS**	**F**	**P**
Cell Age	2	289.899	144.949	20.370	<0.001
Treatment Group	1	9.201	9.201	1.293	0.264
Cell Age x Treatment	2	7.473	3.736	0.525	0.597
Residual	30	213.470	7.116		
Total	35	520.043	14.858		

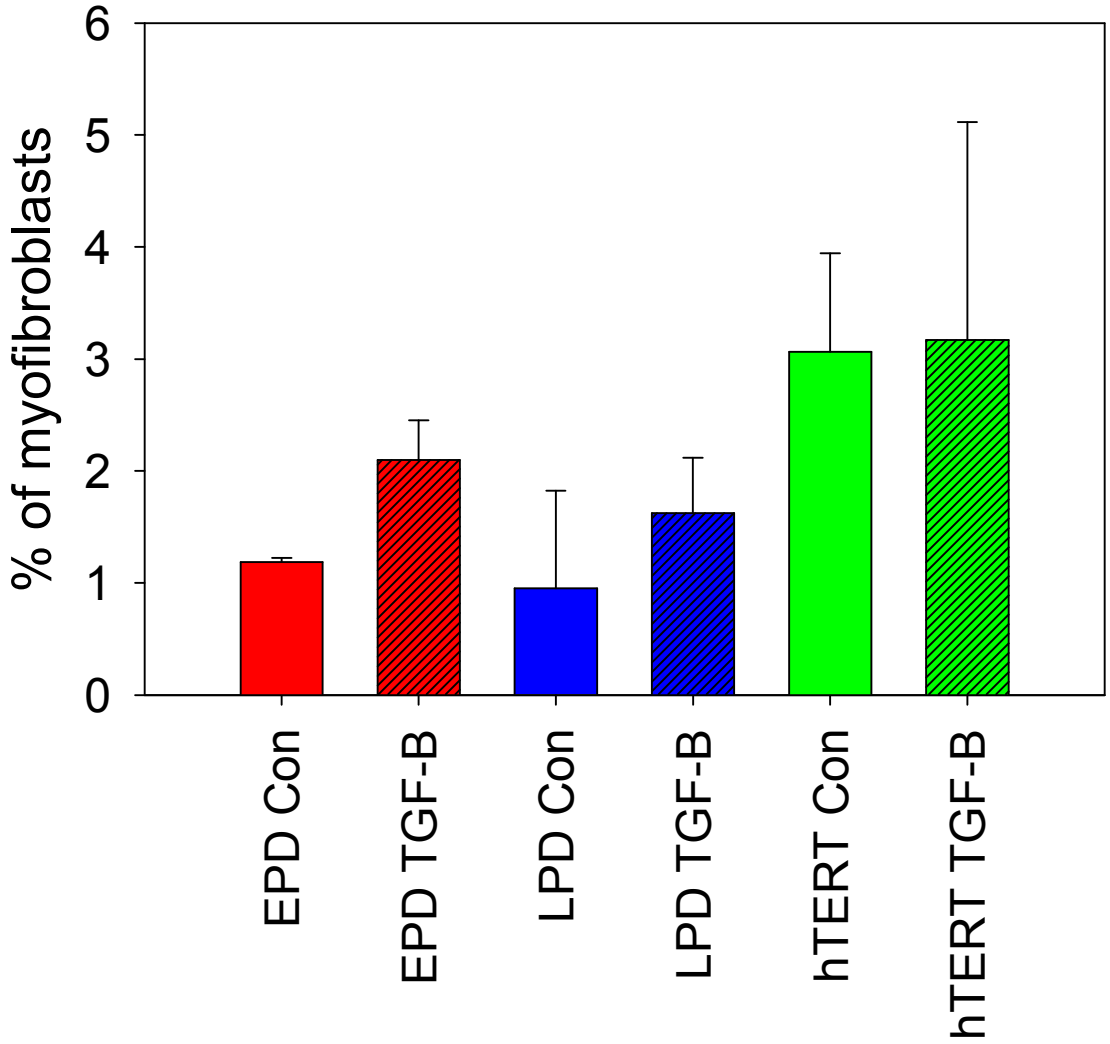

Figure 7. Percentage of myofibroblasts in collagen lattices. Myofibroblast formation was limited in all three cell ages regardless of treatment group and there was no significant difference among any of the groups.

A two-way ANOVA was conducted to evaluate the effects of cell age and TGF-β1 treatment on the development of myofibroblasts. The levels of cell age were early population doubling (EPD), late population doubling (LPD), and the cells transduced with telomerase (hTERT). The levels of treatment were no treatment (control) and TGF-β1 treatment. No significant differences were found in either the cell ages, $F(2,6) = 1.892$, $p = 0.231$, or the treatment, $F(1,6) = 0.756$, $p = 0.418$. Nor was a significant interaction found, $F(2,6) = 0.272$, $p = 0.771$ (Table 3).

Cell Count

The mean number of cells per field of view (fov) was also calculated for the unreleased collagen lattices (Figure 8). In the EPD control group, 366 cells were counted from 10 fov from two lattices yielding a mean of 36.6 cells/fov whereas the TGF-β group had 321 cells in 10 fov from two lattices for a mean of 32.1 cells/fov. The LPD control group had 256 cells counted in 10 fov from two lattices with a mean of 25.6 cells/fov and 278 cells in 10 fov from two lattices giving a mean of 27.8 cells/fov in the TGF-β group. In the hTERT control group, there were 608 cells counted in 10 fov from two lattices to yield a mean of 60.8 cells/fov and 594 cells in 10 fov from two lattices for the TGF-β group giving them a mean of 59.4 cells/fov. Raw data can be found in the Appendix.

A two-way ANOVA was conducted to evaluate the effects of cell age and TGF-β1 treatment on the total number of cells present. The levels of cell age were early population doubling (EPD), late population doubling (LPD), and the cells transduced with telomerase (hTERT). The levels of treatment were no treatment (control) and TGF-β1 treatment (TGF). No significant differences were found in either the cell

Table 3. Two-way ANOVA table for collagen lattice myofibroblast formation. None of the groups have a P value of less than 0.05; therefore there were no significant differences and no interaction.

Source of Variation	**DF**	**SS**	**MS**	**F**	**P**
Cell Type	2	0.00950	0.00475	1.892	0.231
Exp. Group	1	0.00190	0.00190	0.756	0.418
Cell Type x Exp. Group	2	0.00136	0.000682	0.272	0.771
Residual	6	0.0151	0.00251		
Total	11	0.0278	0.00253		

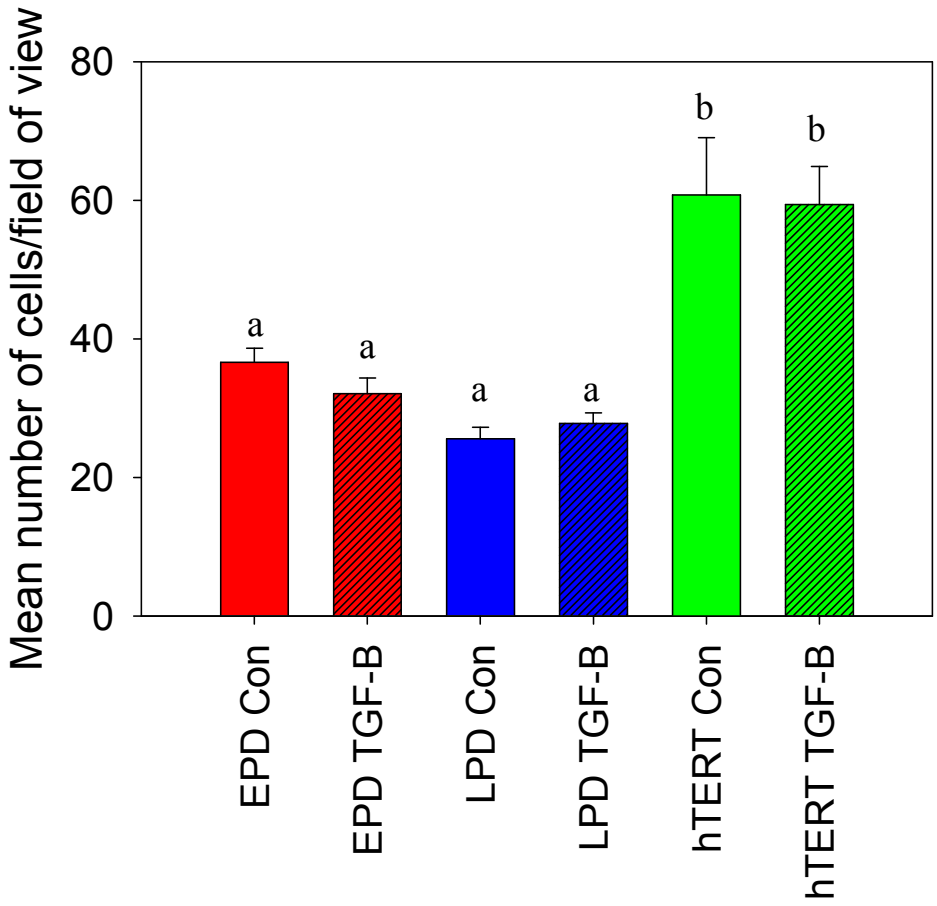

Figure 8. Effect of cell age and treatment on number of cells in collagen lattices. All collagen lattices were originally plated with the same concentration of cells (1.25×10^5 cells). Proliferation effects were estimated by comparing the mean number of cells per field of view observed. EPD and LPD lattices maintained similar cell counts whereas hTERT lattices had a higher number of cells. Bars with the same letter are not significantly different.

ages, $F(2,6) = 1.982$, $p = 0.218$, or the treatment, $F(1,6) = 0.501$, $p = 0.506$, nor was a significant interaction found, $F(2,6) = 0.0901$, $p = 0.915$ (Table 4).

Contraction of Lattices

Contraction of lattices was recorded for collagen lattices that were released from the tissue culture dish. Contractions were recorded at 0, 2, 10, 30 and 60 minute intervals after lattices had been released from the culture dish (Figure 9). Raw data can be found in the Appendix. A two-way ANOVA was run at each of the time intervals to determine the effects of cell ages and treatment.

The two-way ANOVA for the two-minute time interval showed significance for the main effect of cell age, $F(2,66) = 7.874$, $p < 0.001$ (Table 5). No significance was found for the sub effect of TGF-β1 treatment, $F(1,66) = 0.421$, $p = 0.519$. A significant interaction was found between cell age and treatment, $F(2,66) = 14.934$, $p < 0.001$. This interaction was due to differences in the treatment factor on lattice contraction of cells of different ages. The EPD cells had greater lattice contraction in the control group while the hTERT cells showed greater contraction in the TGF-β1group. The LPD cells showed no difference based on treatment.

Fisher LSD across-group tests for the main effect of cell age showed a significant difference in lattice contractions between LPD and the hTERT ($p = 0.002$) and the LPD and EPD ($p < 0.001$). There was a significantly greater lattice contraction for both the EPD and hTERT cells when compared to the LPD cells. The EPD and hTERT cells were not significantly different ($p = 0.705$).

The two-way ANOVA for the ten-minute time interval showed a significance for the main effect of cell age, $F(2,66) = 15.919$, $p < 0.001$ (Table 6). No significance was

Table 4. Two-way ANOVA table for cell number in collagen lattices. A P value less than 0.05 shows significance. None of the groups have a P value of less than 0.05; therefore there were no significant differences and no interaction.

Source of variation	**DF**	**SS**	**MS**	**F**	**P**
Cell Age	2	7.523	3.762	1.982	0.218
Treatment Group	1	0.951	0.951	0.501	0.506
Cell Age x Treatment	2	0.342	0.171	0.0901	0.915
Residual	6	11.39	1.898		
Total	11	20.206	1.837		

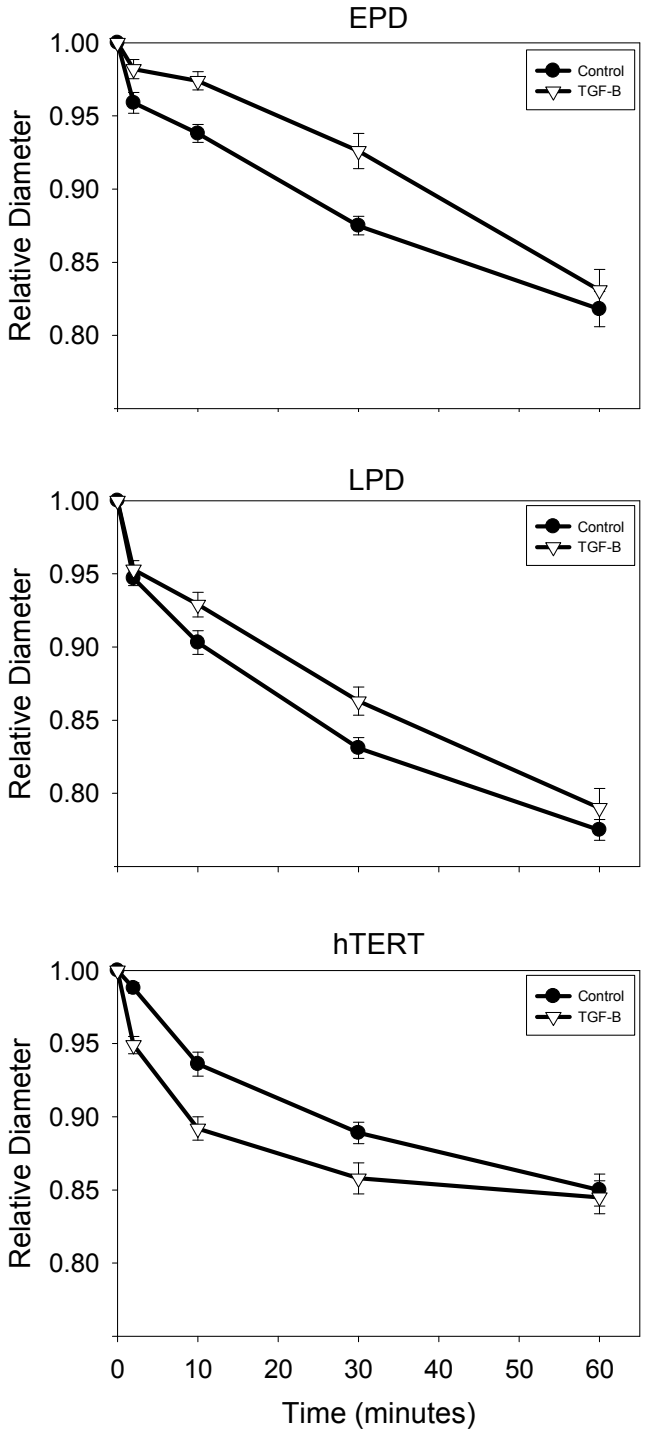

Figure 9. Effect of cell age on lattice contraction in the presence or absence of TGF-β. Lattice contraction graphs showing relative lattice diameter for 2, 10, 30, and 60 minute intervals. Overall the LPD cells contracted the most, followed by the EPD cells and then hTERT cells contracting the least. In lattices with EPD and LPD cells, the control group contracted more than the TGF-β group, whereas in lattices with hTERT cells, the control group contracted less.

Table 5. Two-way ANOVA table for collagen lattice contraction at 2 minutes. A P value less than 0.05 shows significance. There was a significant difference among cell ages but not between treatment groups. There was a significant interaction between cell age and treatment group. A Fisher LSD test showed the lattices with LPD cells were significantly different from the lattices with EPD and hTERT cells.

Source of variation	**DF**	**SS**	**MS**	**F**	**P**
Cell Age	2	0.00633	0.00316	7.874	<0.001
Treatment Group	1	0.00016	0.00016	0.421	0.519
Cell Age x Treatment	2	0.0120	0.00600	14.934	<0.001
Residual	66	0.0265	0.00040		
Total	71	0.0450	0.00063		

Table 6. Two-way ANOVA table for collagen lattice contraction at 10 minutes. A P value less than 0.05 shows significance. There was a significant difference among cell ages but not treatment groups. There was a significant interaction between cell age and treatment group. A Fisher LSD test showed the lattices with EPD cells were significantly different from the lattices with LPD and hTERT cells.

Source of variation	**DF**	**SS**	**MS**	**F**	**P**
Cell Age	2	0.160	0.0799	15.919	<0.001
Treatment Group	1	0.00786	0.00786	1.566	0.215
Cell Age x Treatment	2	0.121	0.0607	12.088	<0.001
Residual	66	0.331	0.00502		
Total	71	0.620	0.00874		

found for the sub effect of TGF-β1 treatment $F(1,66) = 1.566$, $p = 0.215$. A significant interaction was found between cell age and treatment, $F(2,66) = 12.088$, $p < 0.001$. This interaction was again due to differences in the treatment factor on lattice contraction of cells of different ages. The EPD cells had greater lattice contraction in the control group while the hTERT cells showed greater contraction in the TGF-β1 group. The LPD cells showed no difference based on treatment.

Fisher LSD across-group tests for the main effect of cell age showed a significant difference in lattice contractions between EPD and hTERT ($p < 0.001$) and the EPD and LPD ($p < 0.001$). There was a significantly greater lattice contraction for both the LPD and hTERT cells when compared to the EPD cells. The LPD and hTERT cells were not significantly different ($p = 0.705$).

The two-way ANOVA for the thirty-minute time interval showed a significance for the main effect of cell age, $F(2,66) = 17.326$, $p < 0.001$, and the sub effect of TGF-β1 treatment $F(1,66) = 5.606$, $p = 0.021$ (Table 7). A significant interaction was also found, $F(2,66) = 11.274$, $p < 0.001$. This interaction was due to differences in the treatment factor on lattice contraction of cells of different ages. The EPD and LPD cells had greater lattice contraction in the control group while the hTERT cells again showed greater contraction in the TGF-β1 group.

Fisher LSD across-group tests for the main effect of cell age showed a significant difference in lattice contractions between EPD and hTERT, ($p = 0.004$), EPD and LPD ($p < 0.001$) and LPD and hTERT ($p = 0.005$). The LPD cells showed the greatest lattice contraction followed by the hTERT cells and then the EPD cells.

Table 7. Two-way ANOVA table for collagen lattice contraction at 30 minutes. A P value less than 0.05 shows significance. There was a significant difference in cell ages and in treatment groups. There was a significant interaction between cell age and treatment group. A Fisher LSD test showed lattices with all three cell ages were significantly different from each other.

Source of variation	**DF**	**SS**	**MS**	**F**	**P**
Cell Age	2	0.0341	0.0171	17.326	<0.001
Treatment Group	1	0.00552	0.00552	5.606	0.021
Cell Age x Treatment	2	0.0222	0.0111	11.274	<0.001
Residual	66	0.0650	0.00098		
Total	71	0.127	0.00179		

The two-way ANOVA for the sixty-minute time interval showed a significance for the main effect of cell age, $F(2,66) = 16.114$, $p < 0.001$ (Table 8). No significance was found for the sub effect of TGF-β1 treatment $F(1,66) = 0.653$, $p = 0.422$. The interaction was not significant, $F(2,66) = 0.423$, $p = 0.657$.

Fisher LSD across-group tests for the main effect of cell age showed a significant difference in lattice contractions between LPD and the hTERT ($p < 0.001$) and the LPD and EPD ($p < 0.001$). There was a significantly greater lattice contraction for the LPD cells than both the EPD and hTERT cells. The EPD and hTERT cells were not significantly different.

The interaction between cell age and treatment at three time points could be attributed to the differing effects of the treatment in different cell ages. The EPD lattices in the control group contracted significantly more at every time point when compared to the EPD lattices in the TGF-β1 group except for the 60-minute mark. The LPD lattices showed a similar trend having more contraction from the control group at the 10 and 30 minute time points. However, the hTERT lattices showed more contraction at every time point from the TGF-β group rather than from the control group at all but the 60 minute time period.

The absence of an interaction at 60 minutes and the lack of significance for the sub effect of treatment across all time intervals, except the 30-minute point, indicate the main effect of cell age has an effect on the contraction of the lattices. While significance of contraction may change dependent upon cell age, the LPD cells had consistently greater lattice contraction than the EPD and hTERT cells. The significant differences between hTERT and EPD cells varied across time intervals but contraction was not

Table 8. Two-way ANOVA table for collagen lattice contraction at 60 minutes. A P value less than 0.05 shows significance. There was a significant difference in cell ages but not in treatment groups. There was not a significant interaction between cell age and treatment group. A Fisher LSD test showed the lattices with LPD cells were significantly different from the lattices with EPD and hTERT cells.

Source of variation	**DF**	**SS**	**MS**	**F**	**P**
Cell Age	2	0.0528	0.0264	16.114	<0.001
Treatment Group	1	0.00107	0.00107	0.653	0.422
Cell Age x Treatment	2	0.00138	0.00069	0.423	0.657
Residual	66	0.108	0.00164		
Total	71	0.163	0.00230		

significantly different at the sixty-minute interval. While treatment caused an interaction in the earlier intervals, that influence was not seen at 60 minutes suggesting that cell age played the major role in lattice contraction. After one hour of contraction, the LPD lattices showed significantly more contraction (21-23% reduction in lattice diameter) than the EPD (17-18% reduction) or the hTERT (15-16% reduction) lattices (Figure 9).

Scratch Assay

The migration rates of the three cell ages were very similar (Figure 10). Within the first 12 hours, the EPD cells migrated into 56% of the wounded area, the LPD cells filled in 63% of the wound, and the hTERT cells covered 49% of the wound area. By 18 hours, the EPD cells had filled in 75% of the area, and 91% by 24 hours. The LPD cells were able to migrate into 83% of the area by 18 hours and only filled 99% of the area by 24 hours. The hTERT cells covered 81% of the wound after 18 hours and 98% by 24 hours.

A two-way ANOVA was conducted to evaluate the effects of cell age and time on the wound closure area (Table 9). The levels of cell age were early population doubling (EPD), late population doubling (LPD), and cells transduced with telomerase (hTERT). The levels of time are at 12, 18, and 24 hours after wounding. A significant difference was found for the sub effect of time, $F(2,45) = 78.733$, $p < 0.001$. The main effect of cell age was not significant, $F(2,45) = 3.068$, $p = 0.056$. No interaction was found between cell age and time, $F(4,45) = 1.268$, $p = 0.297$.

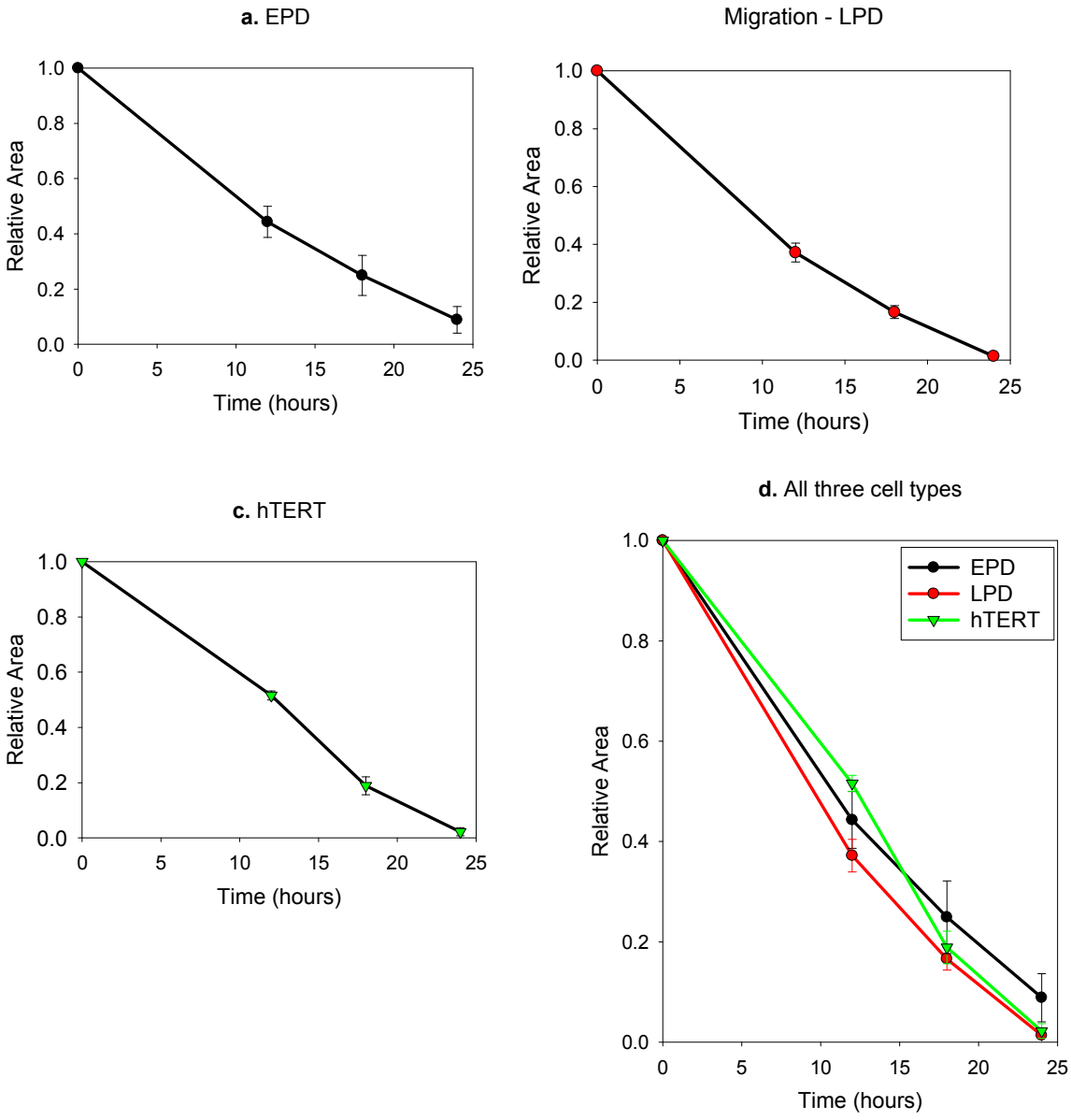

Figure 10. Effect of cell age on migration. Each graph indicates the decreasing size of the wound by plotting the remaining open area. All three cell ages **a.** EPD **b.** LPD and **c.** hTERT when combined on a single diagram **d.** show a similar rate of wound closure.

Table 9. Two-way ANOVA table for scratch assays. A P value greater than 0.05 was obtained when comparing cell type indicating no difference. A P value of less than 0.05 was obtained when comparing the different time points suggesting there is a significant difference. A Fisher LSD test indicated a significant difference between every time point.

Source of Variation	**DF**	**SS**	**MS**	**F**	**P**
Cell Age	2	0.0575	0.0288	3.068	0.056
Time (hours)	2	1.476	0.738	78.733	<0.001
Cell Type x Time	4	0.0475	0.0119	1.268	0.297
Residual	45	0.422	0.00937		
Total	53	2.003	0.0378		

A Fisher LSD test showed that there was a significant difference among all time points with a significant increase in area covered between each time level for all groups, 12 vs. 18, ($p < 0.001$), 12 vs. 24 ($p < 0.001$), and 18 vs. 24 ($p < 0.001$).

DISCUSSION

Previous experiments have demonstrated that TGF-β1 can induce myofibroblast formation on a planar substrate in corneal fibroblasts (Jester et al., 2003), rat dermal fibroblasts (Desmouliere et al., 1993), human lung (Hashimoto et al., 2001) and human dermal fibroblasts (Vaughan et al., 2000). Our results support these observations. It has also been demonstrated that myofibroblasts will differentiate when plated at low densities, in the absence of added growth factors (Masur et al., 1996) so the appearance of myofibroblasts in the control groups as reported in previous experiments (Desmouiere et al. 1993; Vaughan et al., 2000; Robinson and Vaughan, 2007) was expected. For all three cell ages, there was a significant difference between the percent of myofibroblasts in the control group when compared to the percent of myofibroblasts in the TGF-β1 group. So a two-day incubation time was sufficient to favor this differentiation. Yet, when we compared the EPD and LPD cells in either the TGF-β1 group or the control group, there was not a significant difference among the percent of myofibroblasts, suggesting the age of the cell does not affect the amount of myofibroblast differentiation after two days.

The hTERT cells, in the TGF-β1 and the control groups, differed significantly from both the EPD and LPD cells. This shows that the presence of telomerase in a cell does not inhibit the ability of fibroblasts to form myofibroblasts, but may increase differentiation. This contradicts work done with lung fibroblasts where induction of telomerase reduced differentiation of myofibroblasts (Liu et al., 2006) Nevertheless, when comparing the mean number of cells, this two-day time period also allowed for

increased proliferation to occur in at least one cell age group. The hTERT cells showed a significantly higher mean number of cells than both the EPD and LPD cells. Because the mean number of cells within EPD and LPD were similar to each other, if proliferation is occurring in these populations, the rate is similar in both groups. Performing an exact cell count in future studies could help determine if proliferation, cell death, or some combination of the two is occurring within the EPD and LPD cells.

Based on the information from the coverslip experiments, similar results were expected from the collagen lattice assays. Because myofibroblasts are highly contractile (Vaughan et al., 2000), the two-day lattices with TGF-β1 were predicted to contract more due to their higher myofibroblast count. Unexpectedly, in the EPD and LPD cells, the opposite occurred and more contraction was observed in the control groups. The hTERT cells with TGF-β1 had more contraction than the control group; however its overall reduction in lattice size was the least of the three cell ages. Increased levels of myofibroblasts should correlate to an increase in contraction (Vaughan et al., 2000). Surprisingly, our results demonstrated limited myofibroblast differentiation. The largest percent of myofibroblasts formed (3.1-3.2%) were in the hTERT cells, but they showed the least amount of contraction. The ability of cells to contract a lattice can also depend on the number of cells in the lattice: the more cells present, the more likely that contraction will occur (Tomasek et al. 1992). Based on the mean number of cells, the hTERT lattices had significantly higher amounts of cells than the EPD and LPD, but contracted the least. When graphing the cell ages by increasing percentage of contraction, along with mean number of cells and percentage of myofibroblasts, the three cell ages should follow the same trend. However, as the percent of contraction increased, the mean

number of cells and the percentage of myofibroblasts actually decreased (Figure 11). Thus, the effects reported may be a result of some other factor.

One explanation for the unexpected results is the collagen mixture in which the cells were placed. Tension is needed to start the differentiation process (Tomasek et al., 2002) and coverslips provide immediate tension. However, the collagen lattice does not provide tension until the fibroblasts have had a chance to reorganize the lattice (Grinnell, 1994). At 60 minutes, the EPD and LPD lattices were still contracting, whereas the contraction in the hTERT lattices leveled off after about 30 minutes (Figure 9), indicating that tension had yet to be fully generated in the EPD and LPD. Comparing the higher percentage of myofibroblasts formed on the coverslips versus the lower percentage of myofibroblasts in lattices helps to support the idea that tension in the lattices did not fully develop (Figure 12). Therefore, a two-day time period is not enough time for the reorganization of the lattice and differentiation of myofibroblasts. With a longer incubation time, however, cells may proliferate (Grinnell, 2003) and change the total number of cells in the lattice, especially in regard to the hTERT cells thereby creating another variable. Future studies may include ways to reduce these proliferation effects; Ara-C (cytosine arabinoside) has been previously used (Bell et al., 1979)

Another explanation comes from studies of the differentiation process. A two-stage model of myofibroblast formation described by Tomasek et al. (2002) states that after tension is created, the fibroblast differentiates first into a protomyofibroblast. A protomyofibroblast has some contractile force due to the formation of cytoplasmic actin-containing stress fibers. From there, the addition of TGF-β1, along with ED-A fibronectin and more tension, propels the cell into the myofibroblast phenotype. The lattices in this

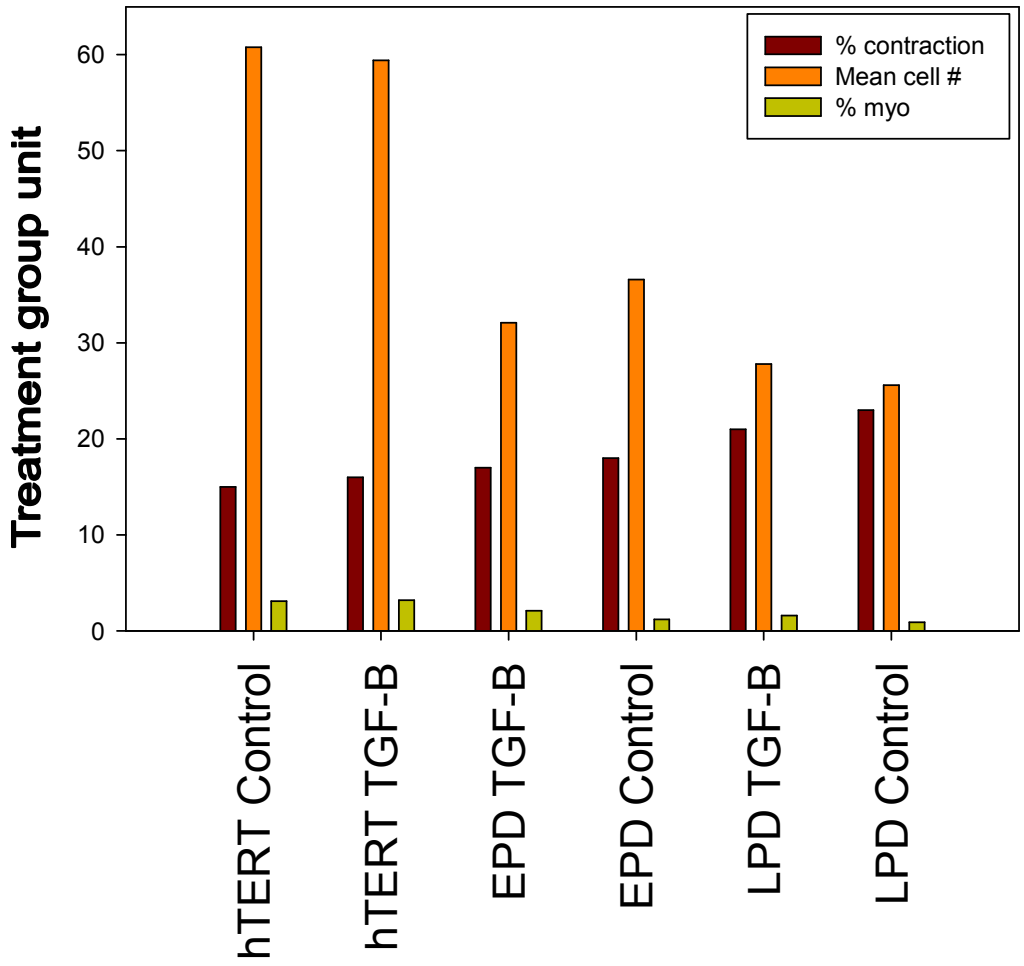

Figure 11. Comparison of contraction, mean cell number and percentage of myofibroblasts for each age of cell. It was expected that all three categories would follow a similar trend. However, as the contraction rate increased, the mean number of cells and percentage of myofibroblasts tended to decrease.

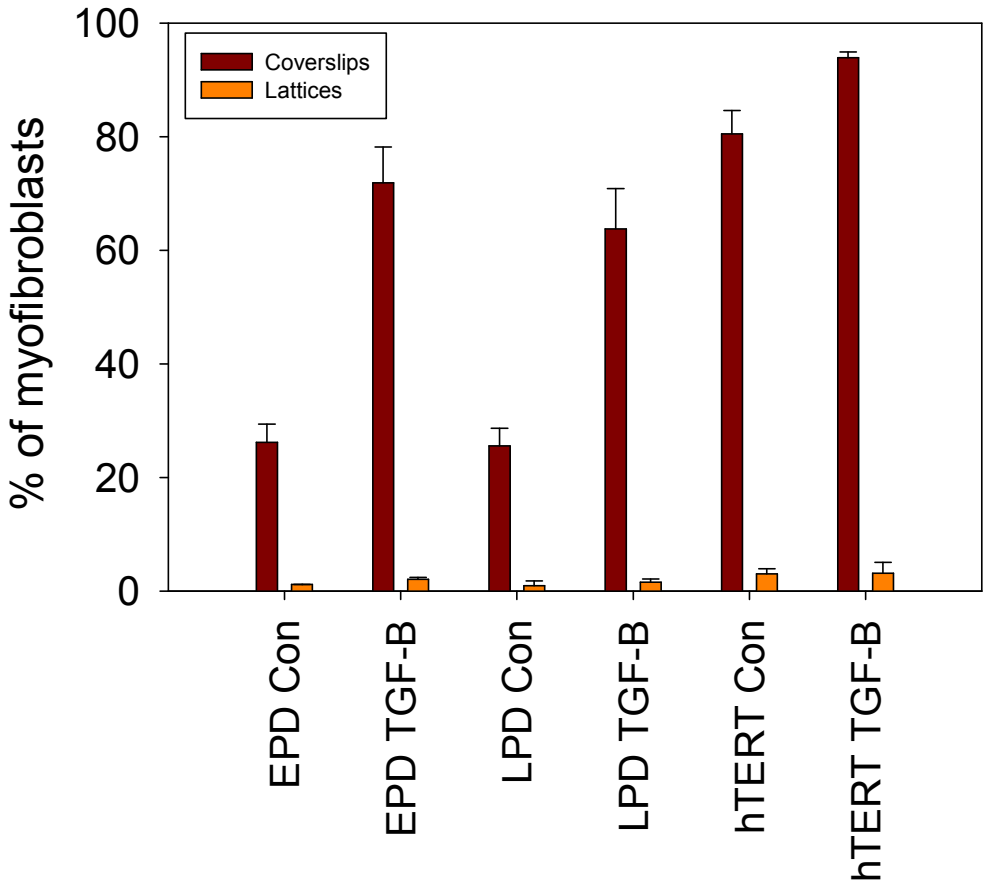

Figure 12. Comparison of percentage of myofibroblasts formed on coverslips and in collagen lattices. Coverslips, as expected, provided an environment for myofibroblast differentiation; however, the collagen lattices were unable to do so.

study may have more cells in the protomyofibroblast stage. Because a protomyofibroblast can generate some contractile force, this limited force could account for the amount of contraction that occurred. TGF-β1 may not promote differentiation until after the protomyofibroblasts have formed. Hence, the lack of contraction from the TGF-β1 groups in the EPD and LPD cell ages may be due to: 1) an insufficient amount of time to allow the formation of protomyofibroblasts, rendering TGF-β1 insignificant at this point or, 2) after stimulation by TGF-β1 the protomyofibroblast may lose some contractile force while becoming a true myofibroblast. Staining for the presence of protomyofibroblasts may help to determine which mechanism contributes to the decreased contraction.

A third option could be the concentration of collagen in the lattices. In prior works by Tomasek (1992) and Vaughan (2000) the collagen concentration was 0.65 mg/mL, and Robinson and Vaughan (2007) used a concentration of 0.60 mg/mL. In this study 0.69 mg/mL was the final concentration and may have created an environment that was harder to contract.

None of the above hypotheses address mean cell number or why the large number of cells in the hTERT lattices had the least amount of contraction. Within the lattices, the distribution of LPD and EPD cells was scattered (Figure 13). The distribution within the hTERT cells, however, was clumped. This clumping may be due to the cells sticking together as they were mixed in the collagen, or the cells could be proliferating without migrating. Either way this clumping of cells may have an effect on the ability of the cells to contract the lattice. Future studies should look at ways to compensate for this

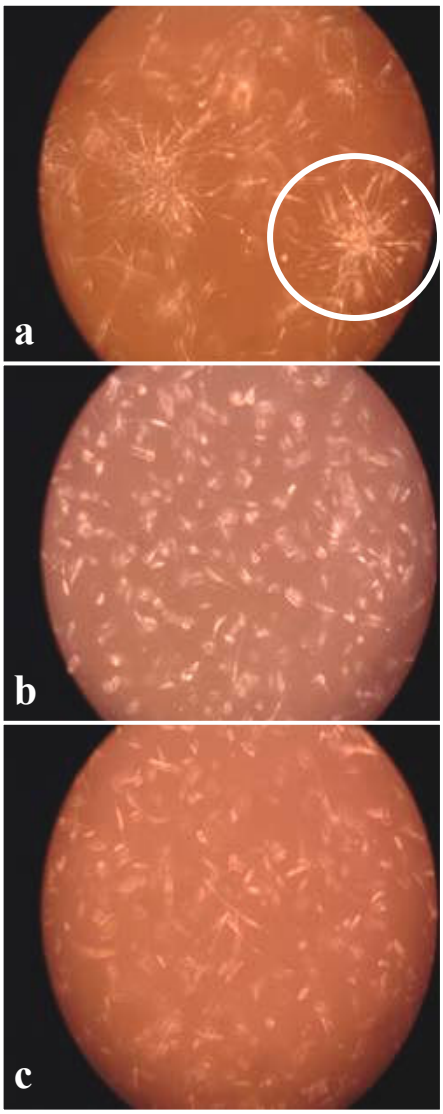

Figure 13. Distribution of cells within collagen lattices. **a.** hTERT cells appeared clumped (as demonstrated within the circle); whereas **b.** EPD cells and **c.** LPD cells appeared to be scattered as single cells.

proliferation by either inhibiting proliferation by CDK inhibitors or doing a dose response assay to find a dose of TGF-β1 that will stop proliferation but still allow differentiation.

Many proliferation inhibitors affect the integrity of the cytoskeleton and cannot be used due to the need for cytoskeletal integrity within the cells (Tomasek et al., 1992). Another option would be to do a final cell count on the hTERT lattices and increase the initial EPD and LPD cell concentrations so that after two days the numbers of cells in all lattices would be similar. Contractile ability could also be measured by the ability of cells to wrinkle a silicone substrate at various stiffness levels (Hinz et al., 2001). This would allow single cell measurements instead of whole-population effects.

The scratch assay did not show any significant differences in migration rates between the three ages of cells. However, there was a significant difference between each time period and the next. This may indicate a consistent rate of migration until the wound is closed. There does not appear to be a time when the cells are moving at a more rapid or at a decreased rate to close in the gaps. Since the GTPases *Ras*, *Rac*, and *Rho* all play a part in cell movement (Nobes and Hall, 1999) the regulation of these enzymes may not be affected by the age of the cell or the expression of telomerase. Analyzing the activity levels of these enzymes during similar studies may help to explain the lack of differences seen in the scratch assays or whether they are affected by age or telomerase. Future studies could also evaluate the migration through collagen substrates that mimic intact collagen fibers, as found in younger skin, and fragmented fibers, as demonstrated in aged skin (Fisher et al., 2009).

The increased proliferation, lack of response in the collagen lattice assay and clumping of the hTERT cells may be due to the expression of telomerase over extended population doublings. The PD of the cells in this study ranged from 145 to 159. When the lattice contractions were compared to previous work done by Robinson and Vaughan (2007), the results were not consistent and the PD of the cells in those studies ranged from 69 to 81. Overexpression of telomerase in CD8 positive t-cells causes an increase in proliferation and sustained overexpression in CD4 and CD8 positive cells promoted genomic instability (Aubert and Lansdorp, 2008). The unusual behavior of the hTERT CT4 cells may be due to the prolonged expression of telomerase. Future studies could investigate the effects of telomerase expression to possibly determine if and when the expression of telomerase starts to have an adverse affect on the cells. Knowing more about the effects of telomerase over time and how cells may change due to a constant expression of telomerase could have an impact on understanding how cells become cancerous since telomerase is expressed in > 90% of tumor samples (Aubert and Lansdorp, 2008). Transient expression of telomerase may be able to rescue a fibroblast from replicative senescence while minimizing the risk of cancer (Steinert et al., 2000). With the increased use of telomeres as a biomarker for aging and their correlation to age-related diseases (von Zglinicki and Martin-Ruiz, 2005), a deeper understanding of telomerase may lead to therapies for some of these diseases.

CONCLUSIONS

TGF-β1 induced myofibroblast differentiation when the cells were placed in an environment with tension regardless of age or telomerase expression. After a two-day period with sufficient tension, the cell age did not affect the percent of myofibroblasts formed, but telomerase did. Myofibroblast formation was limited after a two-day period without sufficient tension, irrespective of age or telomerase expression. Neither cell age nor telomerase expression affected the fibroblasts' ability to migrate into a wounded area. The null hypothesis was that there would be no difference among the three cell ages (early passage, late passage, and hTERT) in the number of myofibroblasts, the ability to contract or migration time. This hypothesis was rejected and the alternate hypothesis that there would be a difference among the cell ages in the number of myofibroblasts, the ability to contract or migration time was accepted. The addition of telomerase increased myofibroblast formation, limited the contraction and had no affect on the migration. Overall, the results showed that replicative senescence did not have an effect on myofibroblast formation or migration, but can affect contraction rate.

REFERENCES

Allsopp RC, Vaziri H, Patterson C, Goldstein S, Younglai EV, Futcher AB, Greider CW, Harley CB. 1992. Telomere length predicts the replicative capacity of human fibroblasts. Natl Acad Sci 89:10114–10118.

Ashcroft GS, Mills SJ, Asworth JJ. 2002. Ageing and wound healing. Biogerentology 3:337-345.

Assoian RK, Komoriya A, Meyers CA, Miller DM, Sporn MB. 1983. Transforming growth factor-beta in human platelets. Identification of a major storage site, purification, and characterization. J Biol Chem 258:7155-60.

Aubert G, Lansdorp PM. 2008. Telomeres and aging. Physiol Rev 88:557-579.

Bell E, Ivarsson B, Merrill C. 1979. Production of a tissue-like structure by contraction of collagen lattices by human fibroblasts of different proliferative potential *in vitro*. Cell Biol 76:1274-1278.

Bodnar AG, Ouellette M, Frolkis M, Holt SE, Chiu C, Morin GB, Harley CB, Shay JW, Lichtsteiner S, Wright WE. 1998. Extension of life-span by introduction of telomerase into normal human cells. Science 279:349.

Border W, Ruoslahti E. 1992. Transforming growth factor-β in disease: the dark side of tissue repair. J Clin Invest 90:1-7.

Boukamp P. 2005. Skin aging: a role for telomerase and telomere dynamics? Curr Mol Med 5:171-177.

Campisi J. 1997. The biology of replicative senescence. Eur J Cancer 33:703-709.

Cawthon RM, Smith KR, O'Brien E, Sivatchenko A, Kerber RA. 2003. Association between telomere length in blood and mortality in people aged 60 years or older. Lancet 361:393–395.

Clark RA. 1989. Wound repair. Curr Opin Cell Biol 1:1000-8.

Cristofalo VJ, Lorenzini A, Allen RG, Torres C, Tresini M. 2004. Replicative senescence: a critical review. Mech Ageing Dev 125:827-848.

Darby I, Skalli O, Gabbiani G. 1990. Alpha-smooth muscle actin is transiently expressed by myofibroblasts during experimental wound healing. Lab Invest 63:21-9.

Denker SP, Barber DL. 2002. Cell migration requires both ion translocation and cytoskeletal anchoring by the Na-H exchanger NHE1. J Cell Bio 159:1087-96.

Desmouliere A. 1995. Factors influencing myofibroblast differentiation during wound healing and fibrosis. Cell Biol Int 19:471-476.

Desmouliere A, Geinoz A, Gabbiani F, Gabbani G. 1993. Transforming growth factor-β1 induces α-smooth muscle actin expression in granulation tissue myofibroblasts and in quiescent and growing cultured fibroblasts. J Cell Biol 122:103-111.

Fisher GJ, Quan T, Purohit T, Shao Y, Cho MK, He T, Varani J, Kang S, Voorhees JJ. 2009. Collagen fragmentation promotes oxidative stress and elevates matrix metalloproteinase-1 in fibroblasts in aged human skin. Am J Pathol 174:101-114.

Fisher GJ, Varani J, Voorhees JJ. 2008. Looking older: fibroblast collapse and therapeutic implications. Arch Dermatol 144:666-72.

Funk WD, Wang CK, Shelton DN, Harley CB, Pagon GD, Hoeffler WK. 2000. Telomerase expression restores dermal integrity to in vitro-aged fibroblasts in a reconstituted skin model. Exp Cell Res 258:270-8.

Gartner LP, Hiatt JL. 2007. Color Textbook of histology. 3rd ed. Pennsylvania: Saunders Elsevier.

Genever P, Wood E, Cunliffe W. 1993. The wounded dermal equivalent offers a simplified model for studying wound repair *in vitro*. Exp Dermatol 2:266-273.

Gibson JM, Milam SB, Klebe RJ. 1989. Late passage cells display an increase in contractile behavior. Mech Ageing Dev 48:101-10.

Grinnell F. 2003. Fibroblast biology in three-dimensional collagen matrices. Trends Cell Biol 13:264-269.

Grinnell F. 1994. Fibroblast, myofibroblasts, and wound contraction. J Cell Biol 124:401-404.

Harley CB, Futcher AB, Greider CW. 1990. Telomeres shorten during ageing of human fibroblasts. Nature 345:458-60.

Hashimoto S, Gon Y, Takeshita I, Matsumoto K, Maruoka S, Horie T. 2001. Transforming growth factor-beta1 induces phenotypic modulation of human lung fibroblasts to myofibroblast through a c-Jun-NH2-terminal kinase-dependent pathway. Am J Respir Crit Care Med 163:152-7.

Hayflick L, Moorehead PS. 1961. The serial cultivation of human diploid cell strains. Exp Cell Res 25:585-621.

Herbig U, Ferreira M, Condel L, Carey D, Sedivy JM. 2006. Cellular senescence in aging primates. Science 311:1257.

Hinz B, Celetta G, Tomasek JJ, Gabbiani G, Chaponnier C. 2001. Alpha-smooth muscle actin expression upregulates fibroblast contractile activity. Mol Bio Cell 12:2730-41.

Holt SE, Wright WE, Shay JW. 1996. Regulation of telomerase activity in immortal cell lines. Mol Cell Biol 16:2932–2939.

Hornsby P. 2007. Telomerase and the aging process. Exp Gerontol 42:575-581.

Jester JV, Huang J, Fisher S, Spiekerman J, Chang JH, Wright WE, Shay JW. 2003. Myofibroblast differentiation of normal human keratocytes and hTERT, extended-life human corneal fibroblasts. Invest Ophth Vis Sci 44:1850-1858.

Jeyapalan JC, Sedivy JM. 2008. Cellular senescence and organismal aging. Mech Ageing Dev 129:467-74.

Jeyapalan JC, Ferreira M, Sedivy JM, Herbig U. 2007. Accumulation of senescent cells in mitotic tissue of aging primates. Mech Ageing Dev 128:36–44.

Kimura M, Barbieri M, Gardner JP, Skurnick J, Cao X, van Riel N, Rizzo M.R, Paolisso G, Aviv A. 2007. Leukocytes of exceptionally old persons display ultra-short telomeres. Am J Physiol Regul Integr Comp Physiol 293: R2210-R2217.

Kono T, Tanii T, Furukawa M, Mizuno N, Kitajima J, Ishii M, Hamada T. 1990. Correlation between Ageing and Collagen Gel Contractility of Human Fibroblasts. Acta Derm Venereol 70:241-244.

Lindsey J, McGill NI, Lindsey LA, Green DK, Cooke HJ. 1991. In vivo loss of telomeric repeats with age in humans. Mutat Res 256:45-8.

Liu T, Hu B, Chung MJ, Ullenbruch M, Jin H, Phan SH. 2006. Telomerase regulation of myofibroblast differentiation. Am J Resp Cell Mol 34:625-633.

Martin P. 1997. Wound healing--aiming for perfect skin regeneration. Science 276:75-81.

Masur SK, Dewal HS, Dinh TT, Erenburg I, Petridou S. 1996. Myofibroblasts differentiate from fibroblasts when plated at low density. Proc Natl Acad Sci 93:4219-4223.

Nobes CD, Hall A. 1999. Rho GTPases control polarity, protrusion, and adhesion during cell movement. J Cell Biol 144:1235-1244.

Ogami M, Ikura Y, Ohsawa M, Matsuo T, Kayo S, Yoshimi N, Hai E, Shirai N, Ehara S, Komatsu R, Naruko T, Ueda M. 2004. Telomere shortening in human coronary artery diseases. Arterioscler Thromb Vasc Biol 24:546–550.

Panossian LA, Porter VR, Valenzuela HF, Zhu X, Reback E, Masterman D, Cummings JL, Effros RB. 2003. Telomere shortening in T cells correlates with Alzheimer's disease status. Neurobiol Aging 24:77–84.

Robinson ED, Vaughan MB. 2007. Replicative senescence affects fibroblast α-smooth muscle actin and contractility. FASEB J 2008 22:980.3.

Shay JW, Wright WE. 2007. Hallmarks of telomeres in ageing research. J Pathol 211:114-123.

Singer AJ, Clark RA. 1999. Cutaneous wound healing. N Engl J Med 341:738-46.

Skalli O, Ropraz P, Trzeciak A, Benzonana G, Gillessen D, Gabbiani G. 1986. A monoclonal antibody against alpha-smooth muscle actin: a new probe for smooth muscle differentiation. J Cell Biol 103:2787-96.

Slagboom PE, Droog S, Boomsma DI. 1994. Genetic determination of telomere size in humans: a twin study of three age groups. Am J Hum Genet 55:876-82.

Steinert S, White DM, Zou Y, Shay JW, Wright WE. 2002. Telomere biology and cellular aging in nonhuman primate cells. Exp Cell Res 272:146–152.

Steinert S, Shay JW, Wright WE. 2000. Transient expression of human telomerase extends the life span of normal human fibroblasts. Biochem Biophys Res Commun 273:1095-8.

Tomasek J, Gabbiani G, Hinz B, Chaponnier C, Brown R. 2002. Myofibroblasts and mechanoregulation of connective tissue remodeling. Nature 3:349-363.

Tomasek J, Haaksma C, Eddy R, Vaughan M. 1992. Fibroblast contraction occurs on release of tension in attached collagen lattices: dependency on an organized actin cytoskeleton and serum. Anat Rec 232:359-68.

Varani J, Dame MK, Rittie L, Fligiel SE, Kang S, Fisher GJ, Voorhees JJ. 2006. Decreased collagen production in chronologically aged skin: roles of age-dependent alteration in fibroblast function and defective mechanical stimulation. Am J Pathol 168:1861-8.

Vaughan MB, Ramirez RD, Brown SA, Yang JC, Wright WE, Shay JW. 2004. A reproducible laser-wounded skin equivalent model to study the effects of aging in vitro. Rejuv Res 7:99-110.

Vaughan MB, Howard E, Tomasek J. 2000. Transforming growth factor-β1 promotes The morphological and functional differentiation of the myofibroblast. Exp Cel Res 257:180-189.

von Zglinicki T, Martin-Ruiz CM, 2005. Telomeres as biomarkers for ageing and age-related diseases. Curr Mol Med 5:197–203.

Wang E, Gundersen D. 1984. Increased organization of cytoskeleton accompanying the aging of human fibroblasts in vitro. Exp Cel Res 154:191-202.

West MD. 1994. The cellular and molecular biology of skin aging. Arch Dermatol 130:87-95.

Wright W, Shay J. 2002. Historical claims and current interpretations of replicative aging. Nat Biotechnol 20:682.

Yamato M, Yamamoto K, Hayashi T. 1992. Decrease in cellular potential of collagen gell contraction due to in vitro cellular aging: a new aging index of fibroblast with high sensitivity. Connect Tissue 24:157-162.

Yang L, Qiu CX, Ludlow A, Ferguson WJ, Brunner G. 1999. Active transforming growth factor-β in wound repair. Am J Pathol 154:105-111.

APPENDIX A

RAW DATA FOR EXPERIMENTS:

1a. Raw data for coverslips: EPD control groups

	fov	number of nuclei	# of a-sma cells	% a-sma		fov	number of nuclei	# of a-sma cells	% a-sma
2 day EPD control 090330	1	8	0	0.000	2 day EPD control 090401	1	8	5	62.500
	2	6	3	50.000		2	8	3	37.500
	3	10	2	20.000		3	9	0	0.000
	4	7	3	42.857		4	9	2	22.222
	5	9	0	0.000		5	10	2	20.000
	6	9	2	22.222		6	10	2	20.000
	7	9	2	22.222		7	5	1	20.000
	8	6	5	83.333		8	9	4	44.444
	9	10	4	40.000		9	13	4	30.769
	10	8	2	25.000		10	6	0	0.000
	11	11	3	27.273		11	8	4	50.000
	12	7	2	28.571		12	10	4	40.000
total		100	28	36.148	total		105	31	34.744
avg		8.3333	2.33333		avg		8.75	2.58333	

	fov	number of nuclei	# of a-sma cells	% a-sma		fov	number of nuclei	# of a-sma cells	% a-sma
2 day EPD control 090506	1	7	0	0.000	2 day EPD control 090506	1	11	0	0.000
	2	10	3	30.000		2	8	0	0.000
	3	10	3	30.000		3	11	2	18.182
	4	7	3	42.857		4	10	0	0.000
	5	11	2	18.182		5	6	2	33.333
	6	8	2	25.000		6	5	1	20.000
	7	10	2	20.000		7	9	1	11.111
	8	7	3	42.857		8	9	2	22.222
	9	8	3	37.500		9	12	2	16.667
	10	9	1	11.111		10	14	4	28.571
	11	8	1	12.500		11	11	2	18.182
	12	11	1	9.091		12	6	1	16.667
total		106	24	27.910	total		112	17	18.494
avg		8.8333	2		avg		9.33333	1.41667	

	fov	number of nuclei	# of a-sma cells	% a-sma		fov	number of nuclei	# of a-sma cells	% a-sma
2 day EPD control 090530	1	10	1	10.000	2 day EPD control 090530	1	11	2	18.182
	2	7	2	28.571		2	13	1	7.692
	3	9	0	0.000		3	11	4	36.364
	4	8	4	50.000		4	10	0	0.000
	5	15	2	13.333		5	12	0	0.000
	6	19	4	21.053		6	10	2	20.000
	7	22	3	13.636		7	12	3	25.000
	8	12	2	16.667		8	13	2	15.385
	9	17	2	11.765		9	8	1	12.500
	10	12	2	16.667		10	14	0	0.000
	11	12	3	25.000		11	12	4	33.333
	12	14	1	7.143		12	6	1	16.667
total		157	26	21.383	total		132	20	18.512
avg		13.083	2.16667		avg		11	1.66667	

1b. Raw date for coverslips: EPD TGF-β groups

	fov	number of nuclei	# of a-sma cells	% a-sma		fov	number of nuclei	# of a-sma cells	% a-sma
2 day EPD TGF-B 090330	1	7	5	71.429	2 day EPD TGF-B 090401	1	9	4	44.444
	2	9	7	77.778		2	7	5	71.429
	3	7	5	71.429		3	8	6	75.000
	4	6	5	83.333		4	5	4	80.000
	5	6	6	100.000		5	7	4	57.143
	6	7	7	100.000		6	6	5	83.333
	7	9	5	55.556		7	6	2	33.333
	8	8	8	100.000		8	8	6	75.000
	9	8	8	100.000		9	5	4	80.000
	10	8	4	50.000		10	6	5	83.333
	11	11	11	100.000		11	7	2	28.571
	12	8	7	87.500		12	6	4	66.667
total		94	78	99.702	total		80	51	77.825
avg		7.8333	6.5		avg		6.66667	4.25	

	fov	number of nuclei	# of a-sma cells	% a-sma		fov	number of nuclei	# of a-sma cells	% a-sma
2 day EPD TGF-B 090506	1	19	8	42.105	2 day EPD TGF-B 090506	1	13	4	30.769
	2	14	7	50.000		2	9	6	66.667
	3	9	7	77.778		3	9	3	33.333
	4	6	3	50.000		4	6	2	33.333
	5	6	4	66.667		5	9	3	33.333
	6	13	5	38.462		6	10	6	60.000
	7	13	6	46.154		7	6	4	66.667
	8	9	6	66.667		8	12	8	66.667
	9	17	9	52.941		9	9	5	55.556
	10	12	5	41.667		10	11	6	54.545
	11	10	5	50.000		11	10	5	50.000
	12	13	7	53.846		12			
total		141	72	63.629	total		104	52	55.087
avg		11.75	6		avg		8.66667	4.33333	

	fov	number of nuclei	# of a-sma cells	% a-sma		fov	number of nuclei	# of a-sma cells	% a-sma
2 day EPD TGF-B 090530	1	12	8	66.667	2 day EPD TGF-B 090530	1	8	5	62.500
	2	12	9	75.000		2	11	10	90.909
	3	23	15	65.217		3	11	7	63.636
	4	16	9	56.250		4	7	5	71.429
	5	12	4	33.333		5	18	14	77.778
	6	11	7	63.636		6	9	4	44.444
	7	7	5	71.429		7	16	11	68.750
	8	8	2	25.000		8	14	8	57.143
	9	13	7	53.846		9	10	2	20.000
	10	8	2	25.000		10	14	6	42.857
	11	20	11	55.000		11	12	4	33.333
	12	11	8	72.727		12	11	6	54.545
total		153	87	66.311	total		141	82	68.733
avg		12.75	7.25		avg		11.75	6.83333	

1c. Raw data for coverslips: LPD control groups

	fov	number of nuclei	# of a-sma cells	% a-sma
2 day LPD control 090330	1	7	0	0.000
	2	16	2	12.500
	3	11	0	0.000
	4	9	1	11.111
	5	15	1	6.667
	6	12	4	33.333
	7	6	1	16.667
	8	12	2	16.667
	9	6	0	0.000
	10	13	0	0.000
	11	15	2	13.333
	12	8	2	25.000
total		130	15	13.528
avg		10.833	1.25	

	fov	number of nuclei	# of a-sma cells	% a-sma
2 day LPD control 090401	1	7	7	100.000
	2	7	4	57.143
	3	8	1	12.500
	4	11	3	27.273
	5	8	3	37.500
	6	5	3	60.000
	7	11	2	18.182
	8	7	0	0.000
	9	8	1	12.500
	10	7	1	14.286
	11	10	0	0.000
	12	9	0	0.000
total		98	25	33.938
avg		8.16667	2.08333	

	fov	number of nuclei	# of a-sma cells	% a-sma
2 day LPD control 090506	1	8	1	12.500
	2	11	3	27.273
	3	6	2	33.333
	4	7	1	14.286
	5	6	1	16.667
	6	7	2	28.571
	7	6	3	50.000
	8	11	0	0.000
	9	5	2	40.000
	10	12	1	8.333
	11	9	3	33.333
	12	5	1	20.000
total		93	20	28.430
avg		7.75	1.66667	

	fov	number of nuclei	# of a-sma cells	% a-sma
2 day LPD control 090506	1	5	1	20.000
	2	5	2	40.000
	3	6	0	0.000
	4	8	2	25.000
	5	8	2	25.000
	6	9	1	11.111
	7	8	1	12.500
	8	9	3	33.333
	9	6	0	0.000
	10	8	0	0.000
	11	12	2	16.667
	12	12	1	8.333
total		96	15	19.194
avg		8	1.25	

	fov	number of nuclei	# of a-sma cells	% a-sma
2 day LPD control 090530	1	12	1	8.333
	2	10	2	20.000
	3	11	1	9.091
	4	18	4	22.222
	5	9	3	33.333
	6	10	2	20.000
	7	11	3	27.273
	8	25	7	28.000
	9	12	4	33.333
	10	15	4	26.667
	11	18	5	27.778
	12	17	7	41.176
total		168	43	29.721
avg		14	3.58333	

	fov	number of nuclei	# of a-sma cells	% a-sma
2 day LPD control 090530	1	8	3	37.500
	2	18	8	44.444
	3	8	3	37.500
	4	16	3	18.750
	5	11	3	27.273
	6	16	2	12.500
	7	15	3	20.000
	8	14	6	42.857
	9	8	0	0.000
	10	12	3	25.000
	11	19	1	5.263
	12	18	3	16.667
total		163	38	28.775
avg		13.5833	3.16667	

1d. Raw data for coverslips: LPD TGF-β groups

	fov	number of nuclei	# of a-sma cells	% a-sma		fov	number of nuclei	# of a-sma cells	% a-sma
2 day LPD TGF-B 090330	1	14	5	35.714	2 day LPD TGF-B 090401	1	9	4	44.444
	2	10	4	40.000		2	6	4	66.667
	3	14	6	42.857		3	6	5	83.333
	4	9	2	22.222		4	11	8	72.727
	5	9	0	0.000		5	6	2	33.333
	6	5	4	80.000		6	6	5	83.333
	7	10	4	40.000		7	5	3	60.000
	8	10	2	20.000		8	8	7	87.500
	9	11	3	27.273		9	6	2	33.333
	10	14	4	28.571		10	7	4	57.143
	11	10	6	60.000		11	6	3	50.000
	12	14	6	42.857		12	6	5	83.333
total		130	46	43.949	total		82	52	75.515
avg		10.833	3.83333		avg		6.83333	4.33333	

	fov	number of nuclei	# of a-sma cells	% a-sma		fov	number of nuclei	# of a-sma cells	% a-sma
2 day LPD TGF-B 090506	1	7	6	85.714	2 day LPD TGF-B 090506	1	7	2	28.571
	2	11	5	45.455		2	7	2	28.571
	3	11	6	54.545		3	9	3	33.333
	4	7	8	114.286		4	7	5	71.429
	5	9	4	44.444		5	11	4	36.364
	6	10	5	50.000		6	6	2	33.333
	7	6	3	50.000		7	6	3	50.000
	8	11	5	45.455		8	6	0	0.000
	9	7	2	28.571		9	8	2	25.000
	10	6	4	66.667		10	12	4	33.333
	11	13	4	30.769		11	11	4	36.364
	12	15	4	26.667		12	12	4	33.333
total		113	56	64.257	total		102	35	40.963
avg		9.4167	4.66667		avg		8.5	2.91667	

	fov	number of nuclei	# of a-sma cells	% a-sma		fov	number of nuclei	# of a-sma cells	% a-sma
2 day LPD TGF-B 090530	1	9	6	66.667	2 day LPD TGF-B 090530	1	11	7	63.636
	2	13	7	53.846		2	11	8	72.727
	3	12	9	75.000		3	10	8	80.000
	4	10	7	70.000		4	11	8	72.727
	5	8	7	87.500		5	15	10	66.667
	6	11	7	63.636		6	13	8	61.538
	7	9	5	55.556		7	7	4	57.143
	8	17	12	70.588		8	14	11	78.571
	9	11	8	72.727		9	9	6	66.667
	10	11	9	81.818		10	8	4	50.000
	11	9	6	66.667		11	8	4	50.000
	12	12	6	50.000		12	11	5	45.455
total		132	89	81.401	total		128	83	76.513
avg		11	7.41667		avg		10.6667	6.91667	

1e. Raw data for coverslips: hTERT control groups

	fov	number of nuclei	# of a-sma cells	% a-sma		fov	number of nuclei	# of a-sma cells	% a-sma
2 day hTERT control 090330	1	20	8	40.000	2 day hTERT control 090401	1	7	6	85.714
	2	30	23	76.667		2	10	9	90.000
	3	13	11	84.615		3	14	10	71.429
	4	15	13	86.667		4	10	9	90.000
	5	24	24	100.000		5	10	10	100.000
	6	31	28	90.323		6	12	12	100.000
	7	21	13	61.905		7	8	7	87.500
	8	21	16	76.190		8	8	8	100.000
	9	13	13	100.000		9	17	17	100.000
	10	22	18	81.818		10	23	10	43.478
total		210	167	79.818	total		119	98	86.812
avg		21	16.7		avg		11.9	9.8	

	fov	number of nuclei	# of a-sma cells	% a-sma		fov	number of nuclei	# of a-sma cells	% a-sma
2 day hTERT control 090506	1	14	13	92.857	2 day hTERT control 090506	1	11	11	100.000
	2	9	9	100.000		2	11	9	81.818
	3	12	11	91.667		3	9	8	88.889
	4	17	13	76.471		4	14	10	71.429
	5	14	13	92.857		5	9	8	88.889
	6	10	10	100.000		6	9	9	100.000
	7	23	22	95.652		7	11	11	100.000
	8	8	6	75.000		8	29	22	75.862
	9	23	21	91.304		9	22	14	63.636
	10	10	10	100.000		10	9	6	66.667
total		140	128	91.581	total		134	108	83.719
avg		14	12.8		avg		13.4	10.8	

	fov	number of nuclei	# of a-sma cells	% a-sma		fov	number of nuclei	# of a-sma cells	% a-sma
2 day hTERT control 090530	1	10	9	90.000	2 day hTERT control 090530	1	12	8	66.667
	2	22	19	86.364		2	31	20	64.516
	3	25	19	76.000		3	38	24	63.158
	4	13	11	84.615		4	24	12	50.000
	5	17	13	76.471		5	26	15	57.692
	6	30	20	66.667		6	13	10	76.923
	7	17	14	82.353		7	21	12	57.143
	8	11	10	90.909		8	20	12	60.000
	9	27	20	74.074		9	26	15	57.692
	10	16	10	62.500		10	21	14	66.667
total		188	145	78.995	total		232	142	62.046
avg		18.8	14.5		avg		23.2	14.2	

1f. Raw data for coverslips: hTERT TGF-β groups

	fov	number of nuclei	# of a-sma cells	% a-sma		fov	number of nuclei	# of a-sma cells	% a-sma
2 day hTERT TGF-B 090330	1	14	11	78.571	2 day hTERT TGF-B 090401	1	12	12	100.000
	2	14	14	100.000		2	7	6	85.714
	3	17	17	100.000		3	19	19	100.000
	4	16	16	100.000		4	21	20	95.238
	5	20	18	90.000		5	13	13	100.000
	6	16	16	100.000		6	8	8	100.000
	7	19	18	94.737		7	27	23	85.185
	8	24	24	100.000		8	16	14	87.500
	9	12	12	100.000		9	7	7	100.000
	10	11	11	100.000		10	9	9	100.000
total		163	157	96.331	total		139	131	95.364
avg		16.3	15.7		avg		13.9	13.1	
	fov	number of nuclei	# of a-sma cells	% a-sma		fov	number of nuclei	# of a-sma cells	% a-sma
2 day hTERT TGF-B 090506	1	14	10	71.429	2 day hTERT TGF-B 090506	1	12	12	100.000
	2	6	5	83.333		2	13	11	84.615
	3	7	6	85.714		3	8	8	100.000
	4	28	27	96.429		4	11	10	90.909
	5	7	7	100.000		5	12	11	91.667
	6	15	14	93.333		6	21	18	85.714
	7	43	41	95.349		7	18	17	94.444
	8	10	8	80.000		8	20	16	80.000
	9	14	13	92.857		9	14	14	100.000
	10	10	10	100.000		10	10	10	100.000
total		154	141	89.844	total		139	127	92.735
avg		15.4	14.1		avg		13.9	12.7	
	fov	number of nuclei	# of a-sma cells	% a-sma		fov	number of nuclei	# of a-sma cells	% a-sma
2 day hTERT TGF-B 090530	1	12	9	75.000	2 day hTERT TGF-B 090530	1	15	14	93.333
	2	15	12	80.000		2	17	16	94.118
	3	16	16	100.000		3	14	13	92.857
	4	18	18	100.000		4	13	13	100.000
	5	13	12	92.308		5	11	11	100.000
	6	16	16	100.000		6	11	11	100.000
	7	10	10	100.000		7	12	12	100.000
	8	15	13	86.667		8	17	15	88.235
	9	29	28	96.552		9	14	14	100.000
	10	12	12	100.000		10	16	15	93.750
total		156	146	93.053	total		140	134	96.229
avg		15.6	14.6		avg		14	13.4	

2a. Raw data for collagen lattice myofibroblast formation: EPD control and TGF-β

	fov	number of nuclei	# of a-sma cells	% a-sma
2 day EPD control 090530	1	33	3	9.091
	2	28	0	0.000
	3	42	1	2.381
	4	29	0	0.000
	5	33	0	0.000
total		165	4	1.147
avg		33	0.8	

	fov	number of nuclei	# of a-sma cells	% a-sma
2 day EPD control 090530	1	41	2	4.878
	2	43	1	2.326
	3	34	1	2.941
	4	48	1	2.083
	5	35	0	0.000
total		201	5	1.223
avg		40.2	1	

	fov	number of nuclei	# of a-sma cells	% a-sma
2 day EPD TGF-B 090530	1	19	1	5.263
	2	28	0	0.000
	3	33	4	12.121
	4	34	0	0.000
	5	28	2	7.143
total		142	7	2.453
avg		28.4	1.4	

	fov	number of nuclei	# of a-sma cells	% a-sma
2 day EPD TGF-B 090530	1	26	1	3.846
	2	39	1	2.564
	3	44	1	2.273
	4	34	2	5.882
	5	36	1	2.778
total		179	6	1.734
avg		35.8	1.2	

2b. Raw data for collagen lattice myofibroblast formation: LPD control and TGF-β

	fov	number of nuclei	# of a-sma cells	% a-sma
2 day LPD control 090530	1	18	2	11.111
	2	26	0	0.000
	3	22	0	0.000
	4	28	2	7.143
	5	20	0	0.000
total		114	4	1.825
avg		22.8	0.8	

	fov	number of nuclei	# of a-sma cells	% a-sma
2 day LPD control 090530	1	27	0	0.000
	2	25	2	8.000
	3	32	0	0.000
	4	35	0	0.000
	5	23	0	0.000
total		142	2	0.800
avg		28.4	0.4	

	fov	number of nuclei	# of a-sma cells	% a-sma
2 day LPD TGF-B 090530	1	32	1	3.125
	2	23	1	4.348
	3	29	1	3.448
	4	39	1	2.564
	5	26	2	7.692
total		149	6	2.118
avg		29.8	1.2	

	fov	number of nuclei	# of a-sma cells	% a-sma
2 day LPD TGF-B 090530	1	23	0	0.000
	2	28	1	3.571
	3	26	1	3.846
	4	26	0	0.000
	5	26	1	3.846
total		129	3	1.126
avg		25.8	0.6	

2c. Raw data for collagen lattice myofibroblast formation: hTERT control and TGF-β

	fov	number of nuclei	# of a-sma cells	% a-sma
2 day hTERT control 090530	1	65	7	10.769
	2	36	4	11.111
	3	69	3	4.348
	4	41	2	4.878
	5	120	10	8.333
total		331	26	3.944
avg		66.2	5.2	

	fov	number of nuclei	# of a-sma cells	% a-sma
2 day hTERT control 090530	1	65	0	0.000
	2	46	4	8.696
	3	80	5	6.250
	4	55	2	3.636
	5	31	1	3.226
total		277	12	2.181
avg		55.4	2.4	

	fov	number of nuclei	# of a-sma cells	% a-sma
2 day hTERT TGF-B 090530	1	57	3	5.263
	2	51	4	7.843
	3	58	3	5.172
	4	37	9	24.324
	5	82	7	8.537
total		285	26	5.114
avg		57	5.2	

	fov	number of nuclei	# of a-sma cells	% a-sma
2 day hTERT TGF-B 090530	1	62	2	3.226
	2	43	0	0.000
	3	62	1	1.613
	4	48	1	2.083
	5	94	5	5.319
total		309	9	1.224
avg		61.8	1.8	

3a. Raw data for collagen lattice reduction: EPD control and TGF-β groups

EX 090530 - EPD		Lattice Size (mm)					Relative Lattice Diameter				
treatment	dish	0	2	10	30	60	0	2	10	30	60
TGF	4	14.75	14	14	13	11	1	0.949	0.949	0.881	0.746
TGF	6	15	15	15	14	12.5	1	1.000	1.000	0.933	0.833
TGF	8	15.5	14.5	14.5	13.5	11.5	1	0.935	0.935	0.871	0.742
TGF	10	15.5	15	15	14.5	13	1	0.968	0.968	0.935	0.839
TGF	12	15.5	15.5	15.25	14	12.75	1	1.000	0.984	0.903	0.823
TGF	16	15	15	14.5	13	12	1	1.000	0.967	0.867	0.800
Control	3	16.5	15.75	15.5	14	12.5	1	0.955	0.939	0.848	0.758
Control	5	15.5	15.5	15.5	14.5	13.5	1	1.000	1.000	0.935	0.871
Control	7	16.5	15.5	15.5	14.5	13	1	0.939	0.939	0.879	0.788
Control	9	15.25	14.5	14.5	13.5	12	1	0.951	0.951	0.885	0.787
Control	13	15.5	15	14.5	13.5	12.5	1	0.968	0.935	0.871	0.806
Control	15	15.5	15	14.5	13.5	12.5	1	0.968	0.935	0.871	0.806

EX 090615 -EPD		Lattice Size (mm)					Relative Lattice Diameter				
treatment	dish	0	2	10	30	60	0	2	10	30	60
TGF	2	15	15	15	14.5	13	1	1.000	1.000	0.967	0.867
TGF	4	15.25	15.25	15	14.5	13	1	1.000	0.984	0.951	0.852
TGF	6	15.75	15.5	15	14.5	13	1	0.984	0.952	0.921	0.825
TGF	8	15.5	15	15	15	14	1	0.968	0.968	0.968	0.903
TGF	10	15	15	15	15	13	1	1.000	1.000	1.000	0.867
TGF	14	14.25	14	14	13	12.5	1	0.982	0.982	0.912	0.877
Control	3	15	15	14	13	12	1	1.000	0.933	0.867	0.800
Control	5	15.5	15	14.25	13.5	14	1	0.968	0.919	0.871	0.903
Control	7	15.25	14	14	13	12	1	0.918	0.918	0.852	0.787
Control	11	14.5	13.5	13.5	12.75	12	1	0.931	0.931	0.879	0.828
Control	13	14	13.5	13	12.25	12	1	0.964	0.929	0.875	0.857
Control	15	14.5	13.75	13.5	12.5	12	1	0.948	0.931	0.862	0.828

3b. Raw data for collagen lattice reduction: LPD control and TGF-β groups

EX 090530 - LPD		Lattice Size (mm)					Relative Lattice Diameter				
treatment	dish	0	2	10	30	60	0	2	10	30	60
TGF	2	15.5	15	15	14	13	1	0.968	0.968	0.903	0.839
TGF	6	15	14.5	14	13	12	1	0.967	0.933	0.867	0.800
TGF	8	14.75	14	14	13	11.5	1	0.949	0.949	0.881	0.780
TGF	10	16	15.5	15.5	13.75	12.5	1	0.969	0.969	0.859	0.781
TGF	12	15.75	15	15	13.5	12	1	0.952	0.952	0.857	0.762
TGF	16	15	14.75	14	12.5	11.25	1	0.983	0.933	0.833	0.750
Control	1	15.5	15	14.5	13	12	1	0.968	0.935	0.839	0.774
Control	5	15.5	14.5	14.5	13.5	12.5	1	0.935	0.935	0.871	0.806
Control	7	16	15	14.75	13	12	1	0.938	0.922	0.813	0.750
Control	9	15.5	14.5	14	13	11.5	1	0.935	0.903	0.839	0.742
Control	11	15.75	15	14.5	13.5	12.5	1	0.952	0.921	0.857	0.794
Control	15	15.25	15	14	13	12	1	0.984	0.918	0.852	0.787

EX 090615 -LPD		Lattice Size (mm)					Relative Lattice Diameter				
treatment	dish	0	2	10	30	60	0	2	10	30	60
TGF	3	15.75	15	15	14	14	1	0.952	0.952	0.889	0.889
TGF	5	15.25	14.5	13.5	13.5	11.5	1	0.951	0.885	0.885	0.754
TGF	7	15.5	14.5	14	14	13	1	0.935	0.903	0.903	0.839
TGF	9	15	14	13.5	12	11	1	0.933	0.900	0.800	0.733
TGF	11	15	14.5	13.5	13	12	1	0.967	0.900	0.867	0.800
TGF	15	16	14.5	14.5	13	12	1	0.906	0.906	0.813	0.750
Control	2	15.25	14.5	14	12.5	12	1	0.951	0.918	0.820	0.787
Control	6	15	14	13	12	12	1	0.933	0.867	0.800	0.800
Control	8	15	14	13	12	11.5	1	0.933	0.867	0.800	0.767
Control	10	15	14	13	12	11	1	0.933	0.867	0.800	0.733
Control	14	14.5	14	13.25	12	11	1	0.966	0.914	0.828	0.759
Control	16	15	14	13	12.75	12	1	0.933	0.867	0.850	0.800

3c. Raw data for collagen lattice reduction: hTERT control and TGF-β groups

EX 090530 - hTERT		Lattice Size (mm)					Relative Lattice Diameter				
treatment	dish	0	2	10	30	60	0	2	10	30	60
TGF	4	15.5	15	14.5	14	14	1.000	0.968	0.935	0.903	0.903
TGF	6	15	14	13	12.5	12	1.000	0.933	0.867	0.833	0.800
TGF	10	16	15	14	13	13	1.000	0.938	0.875	0.813	0.813
TGF	12	15.5	14.5	13.5	12.5	12.5	1.000	0.935	0.871	0.806	0.806
TGF	14	15.25	14.5	13.5	13	12.5	1.000	0.951	0.885	0.852	0.820
TGF	16	15.5	15	14	13.5	13.5	1.000	0.968	0.903	0.871	0.871
Control	3	15	15	14	13	13	1.000	1.000	0.933	0.867	0.867
Control	7	15.75	15.5	15.5	14.5	14.5	1.000	0.984	0.984	0.921	0.921
Control	9	15	14.75	14	12.75	12	1.000	0.983	0.933	0.850	0.800
Control	11	14.5	14.5	14.5	13	13	1.000	1.000	1.000	0.897	0.897
Control	13	14.5	14.5	13.5	13.5	12.5	1.000	1.000	0.931	0.931	0.862
Control	15	15.5	15.25	14.5	13.5	12.5	1.000	0.984	0.935	0.871	0.806

EX 090615 -hTERT		Lattice Size (mm)					Relative Lattice Diameter				
treatment	dish	0	2	10	30	60	0	2	10	30	60
TGF	2	14.75	13.5	12.5	12	12	1.000	0.915	0.847	0.814	0.814
TGF	6	14.5	14	13	13	12	1.000	0.966	0.897	0.897	0.828
TGF	8	15.25	15	14	14	14	1.000	0.984	0.918	0.918	0.918
TGF	10	15	14.5	13.5	13	13	1.000	0.967	0.900	0.867	0.867
TGF	12	15.5	14.5	13.5	13.25	13	1.000	0.935	0.871	0.855	0.839
TGF	16	15	14	14	13	13	1.000	0.933	0.933	0.867	0.867
Control	3	15	14.75	14	13	13	1.000	0.983	0.933	0.867	0.867
Control	5	15	14.5	13.75	13.5	13	1.000	0.967	0.917	0.900	0.867
Control	7	15	15	13.75	13.75	12.5	1.000	1.000	0.917	0.917	0.833
Control	9	15	14.5	13.5	13	12	1.000	0.967	0.900	0.867	0.800
Control	11	15	15	14	13.5	12.5	1.000	1.000	0.933	0.900	0.833
Control	15	14.75	14.5	13.5	13	12.5	1.000	0.983	0.915	0.881	0.847

4. Raw Data for Scratch Assays

EX 090530		Area (mm^2)				Relative Area			
cell type	area	0	12	18	24	0	12	18	24
EPD	1A	0.25	0.13	0.033	0	1	0.52	0.132	0
EPD	2A	0.201	0.035	0	0	1	0.174129	0	0
EPD	3B	0.191	0.085	0.078	0.028	1	0.445026	0.408377	0.146597
LPD	1A	0.271	0.129	0.042	0.022	1	0.476015	0.154982	0.081181
LPD	2B	0.272	0.09	0.049	0	1	0.330882	0.180147	0
LPD	3A	0.149	0.04	0.03	0	1	0.268456	0.201342	0
hTERT	1A	0.375	0.181	0.046	0	1	0.482667	0.122667	0
hTERT	2B	0.349	0.165	0.067	0	1	0.472779	0.191977	0
hTERT	3A	0.378	0.192	0.092	0.032	1	0.507937	0.243386	0.084656

EX 090529		Area (mm^2)				Relative Area			
cell type	area	0	12	18	24	0	12	18	24
EPD	1B	0.237	0.127	0.112	0.07	1	0.535865	0.472574	0.295359
EPD	2B	0.202	0.089	0.037	0	1	0.440594	0.183168	0
EPD	3B	0.222	0.12	0.066	0.02	1	0.540541	0.297297	0.09009
LPD	1A	0.223	0.093	0.031	0	1	0.41704	0.139013	0
LPD	2A	0.268	0.114	0.064	0	1	0.425373	0.238806	0
LPD	3B	0.31	0.097	0.025	0	1	0.312903	0.080645	0
hTERT	1A	0.248	0.14	0.03	0.012	1	0.564516	0.120968	0.048387
hTERT	2B	0.223	0.113	0.071	0	1	0.506726	0.318386	0
hTERT	3B	0.254	0.143	0.034	0	1	0.562992	0.133858	0